

Emergent states of interacting electrons on triangular lattices

Kazushi Kanoda
Applied Physics, University of Tokyo

Spin liquid

- 1. Quantum spin liquid** - κ -(ET)₂Cu₂(CN)₃
 - present status of experiments
 - 2. Doped quantum spin liquid** - κ -(ET)₄Hg_{2.89}Hg₈ -
 - non-FL to FL crossover
 - quantum critical phase
 - BEC-BCS crossover
 - reduced superfluid density
 - preformed pairs & pairing symmetry
- PR X 12_011016 (2022)
arXiv:2201.10714
arXiv:2202.06032
arXiv:2205.03682

Charge glass

- 3. Quantum charge glass** - θ -(ET)₂X -
 - classical manifestations (slow dynamics, aging, short-range order)
 - anomalously high crystallization speed
 - classical to quantum crossover
- arXiv:2201.04855
arXiv:2205.10795

Today's talk is based on collaboration with

K. Miyagawa, Kagawa, Shimizu, Kurosaki, Furukawa, H. Oike, M. Urai, Y. Suzuki,
K. Wakamatsu, Y. Ueno, T. Fujii, J. Ibuka, T. Sato, H. Murase (U Tokyo)

G, Saito, M. Maesato (Kyoto U.)

T. Sasaki, S. Iguchi, M. Saito (Tohoku U., IMR)

R. Kato (RIKEN)

H. Taniguchi, M. Ito (Saitama U.)

S. Yamashita, Y. Nakazawa (Osaka)

F. Pratt (Rutherford-Appleton)

Y. Kohama, A. Miyake, T. Nomura (ISSP)

B. Mikche, M. Dressel (Stuttgart U.)

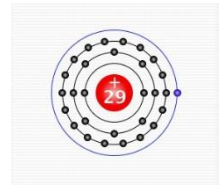
H. Mori (ISSP)

M. Tamura (Tokyo Sci. Univ.)

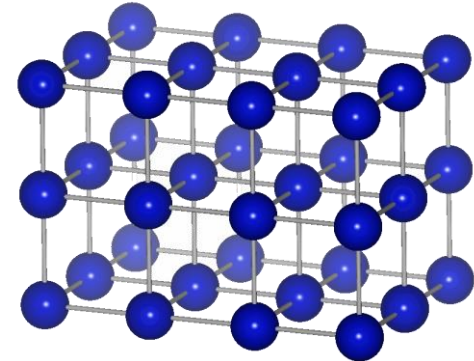
Organic materials → flexible & controllable lattice geometry

Inorganic materials

atom

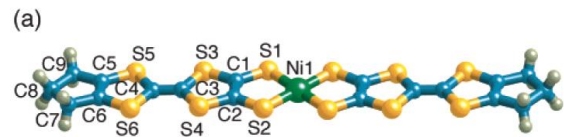


lattice



Orbital degeneracy
Spin-orbit coupling
Hunt coupling
.....

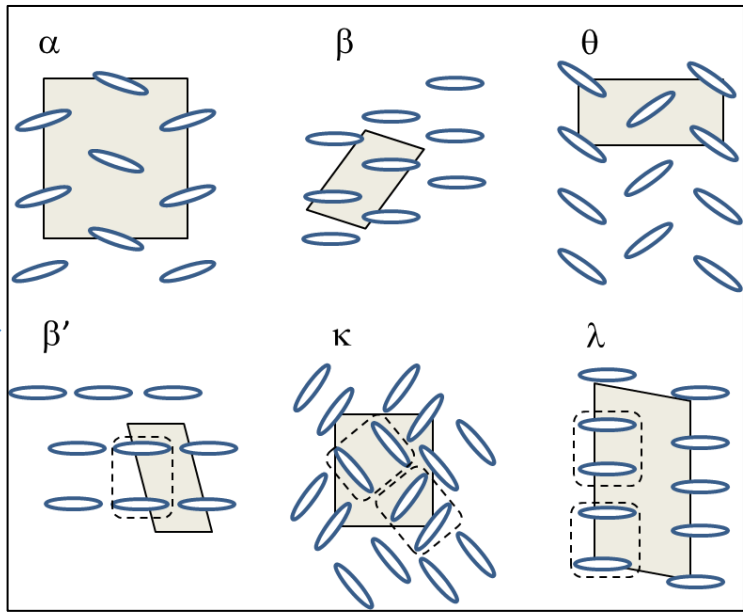
Organic materials



Frontier orbital
(K. Fukui)

lattice

Kino-Fukuyama



Organic materials → Physics of interaction and geometry

Various in-plane structures



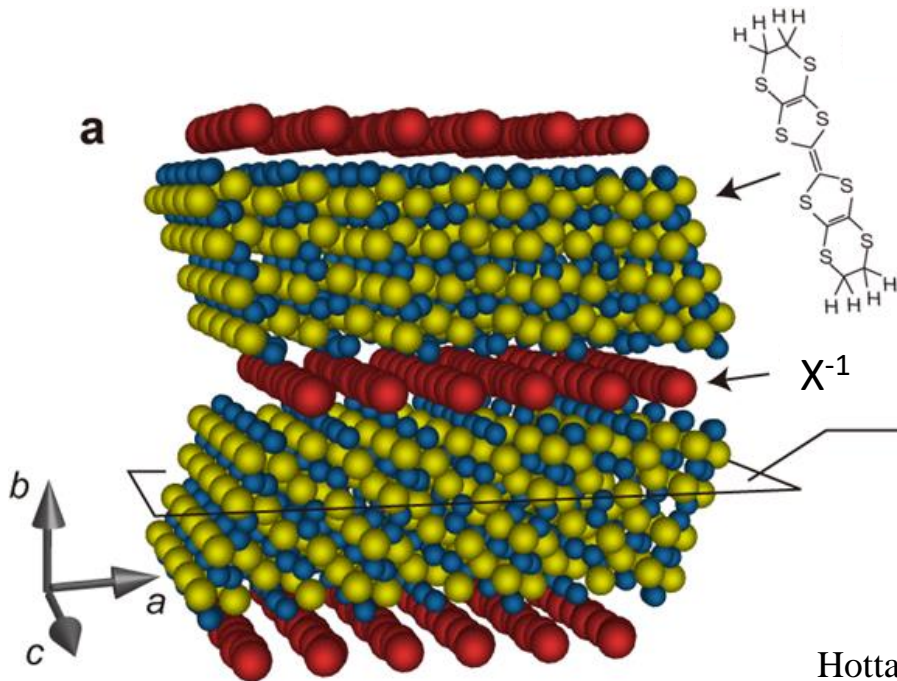
Diverse correlation phenomena



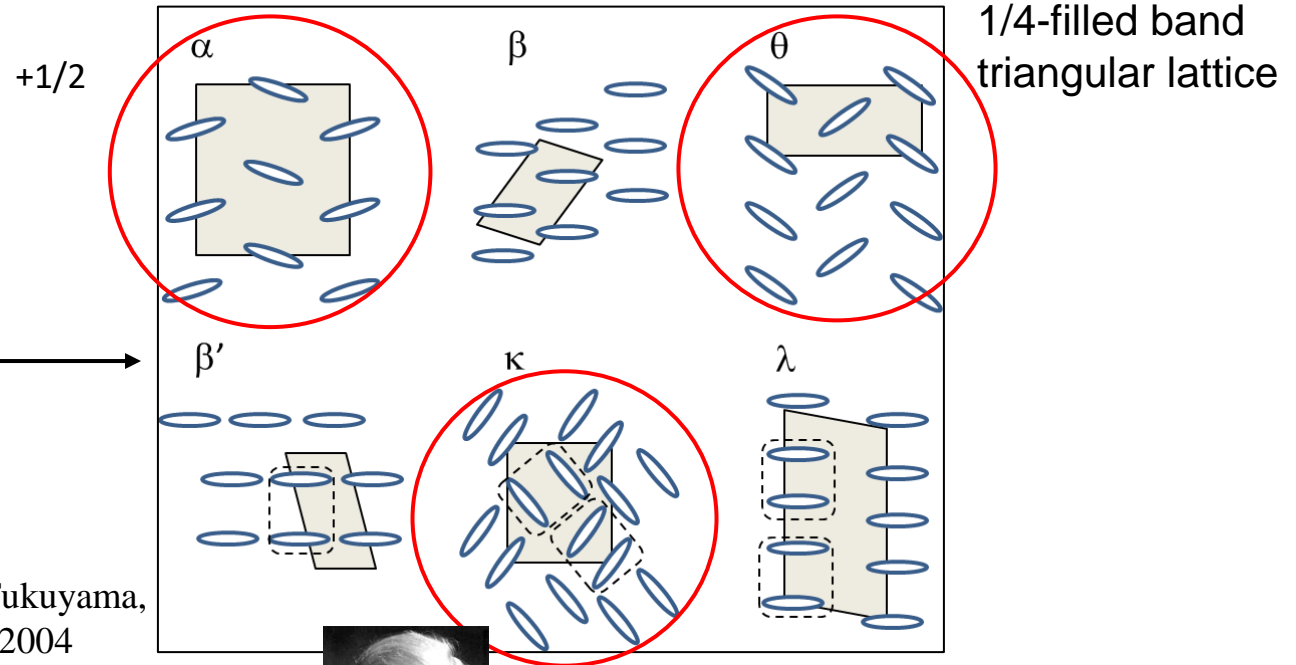
Massless Dirac ele.



Wigner Xtal/glass



Hotta, Seo, Fukuyama,
Chem. Rev., 2004



Mott physics

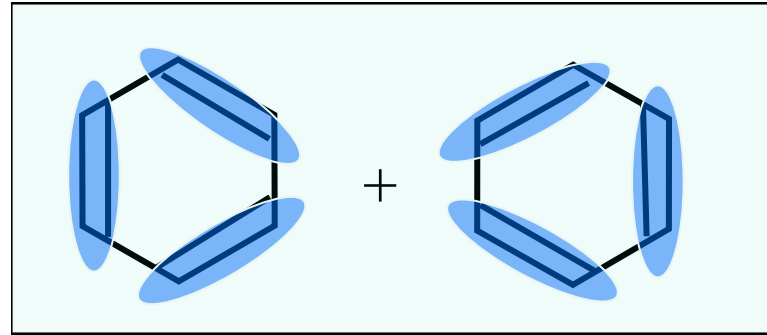
1/2-filled band
triangular lattice

Resonating valence bond (RVB) state as a QSL

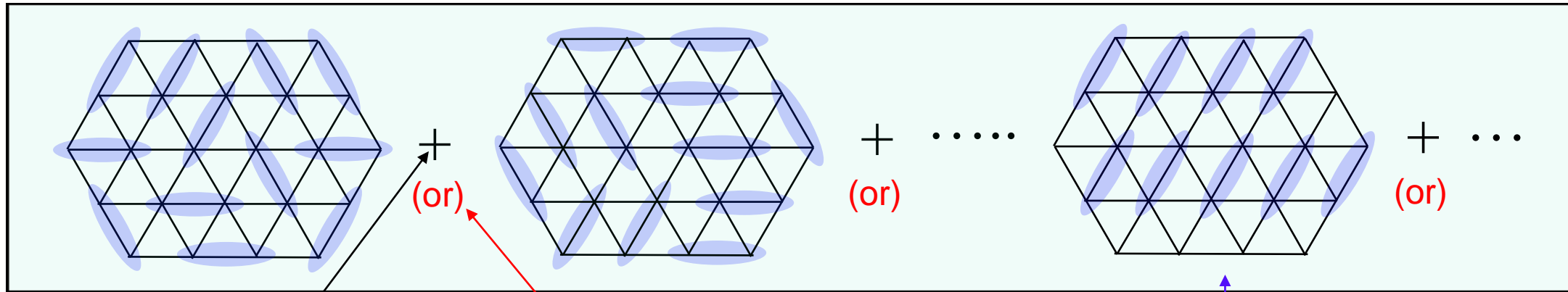


P. W. Anderson

benzene



Triangular
lattice



RVB

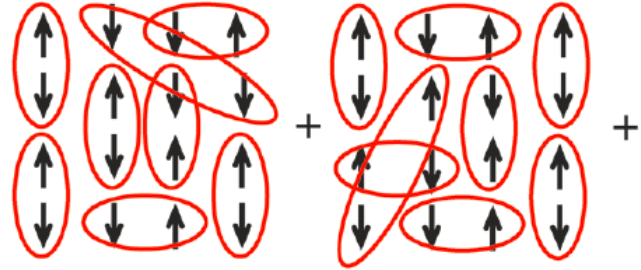
VBG
(Valence bond glass)

VBC (or VBS)
(valence bond crystal (or solid))

Possible variation of QSLs

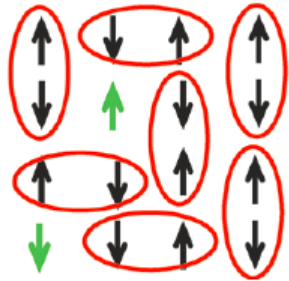
(according to Ogata)

(P_G : projection operator to remove double occupancies)



$$|RVB\rangle = P_G |BCS\rangle \quad \text{gapped}$$

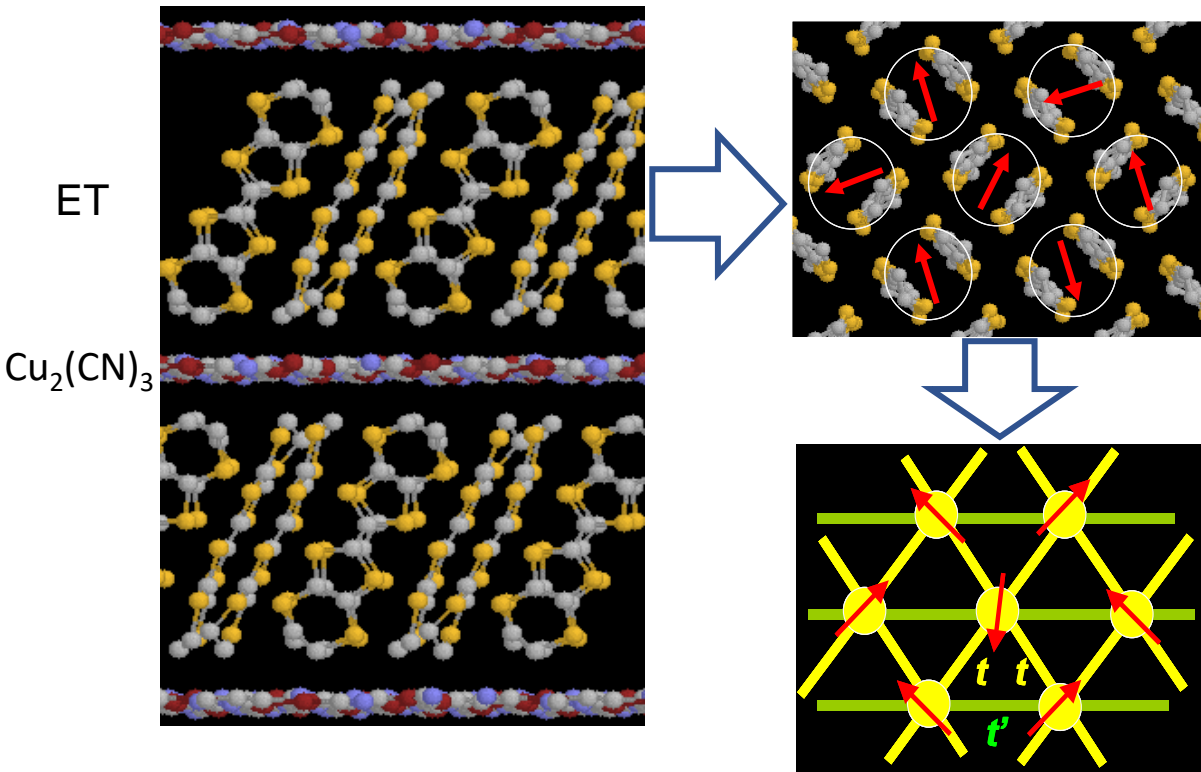
$$|\text{spinon FS}\rangle = P_G |BCS; \Delta \rightarrow 0\rangle \quad \text{gapless}$$



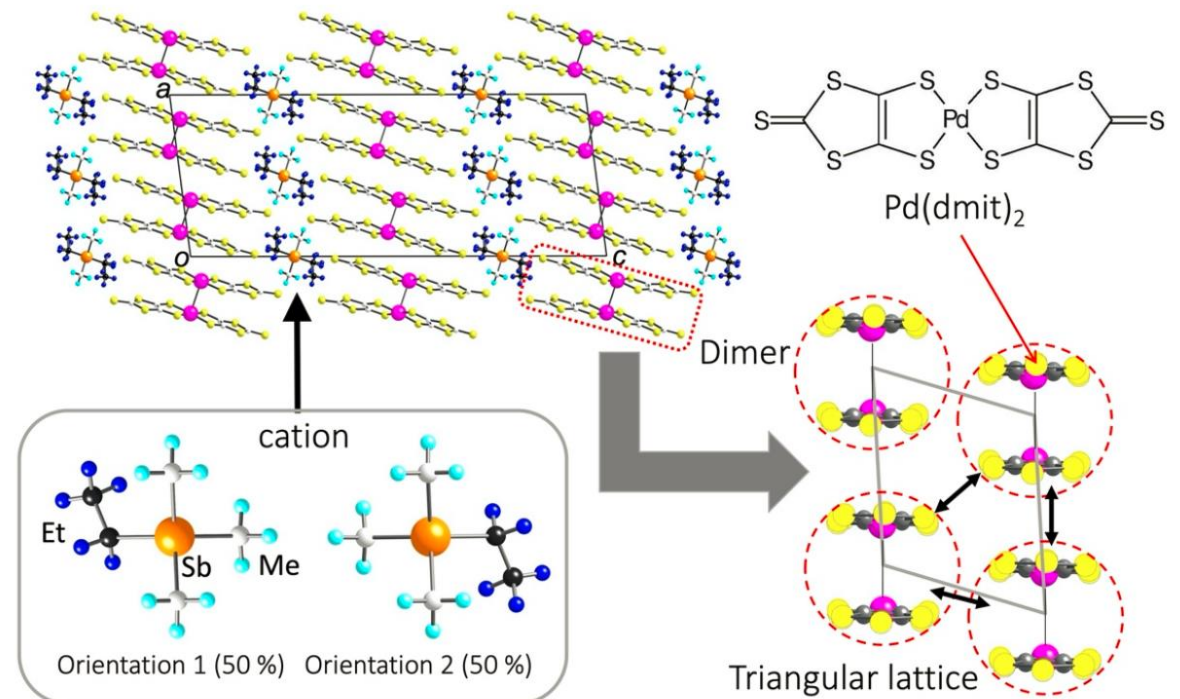
$$|\text{spinon Dirac cone}\rangle = P_G |nodal BCS\rangle \quad \text{gapless (Dirac point)}$$

$$|\text{Chiral spin liquid}\rangle = P_G |chiral SC\rangle \quad (?) \quad \text{gapped}$$

Quantum spin liquid (QSL) candidates with a triangular lattice

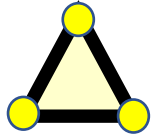


Kato, RIKEN



QSL manifestations

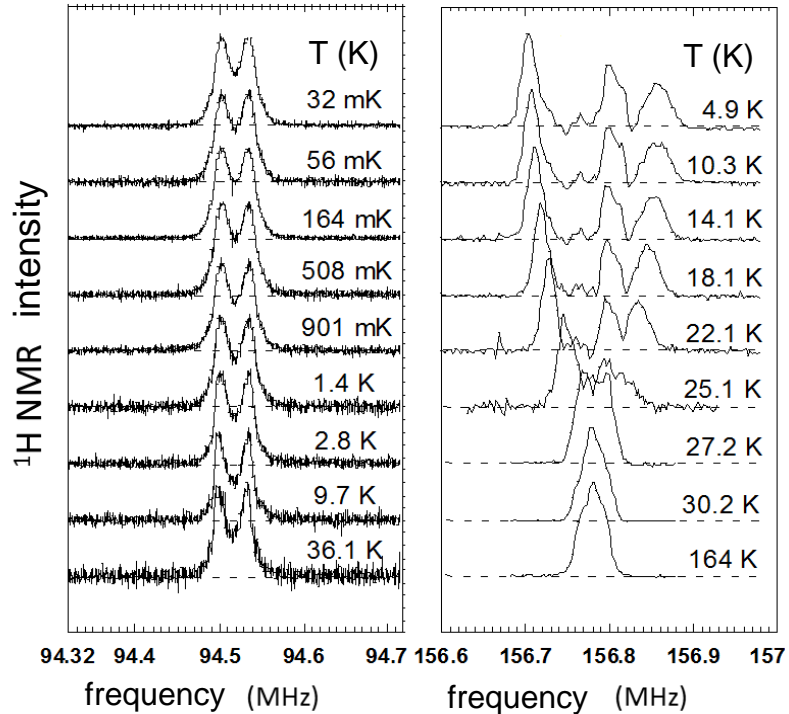
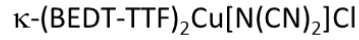
^1H NMR spectra



Triangular lattice



Deformed triangular lattice



No magnetic order



QSL !

Magnetic order

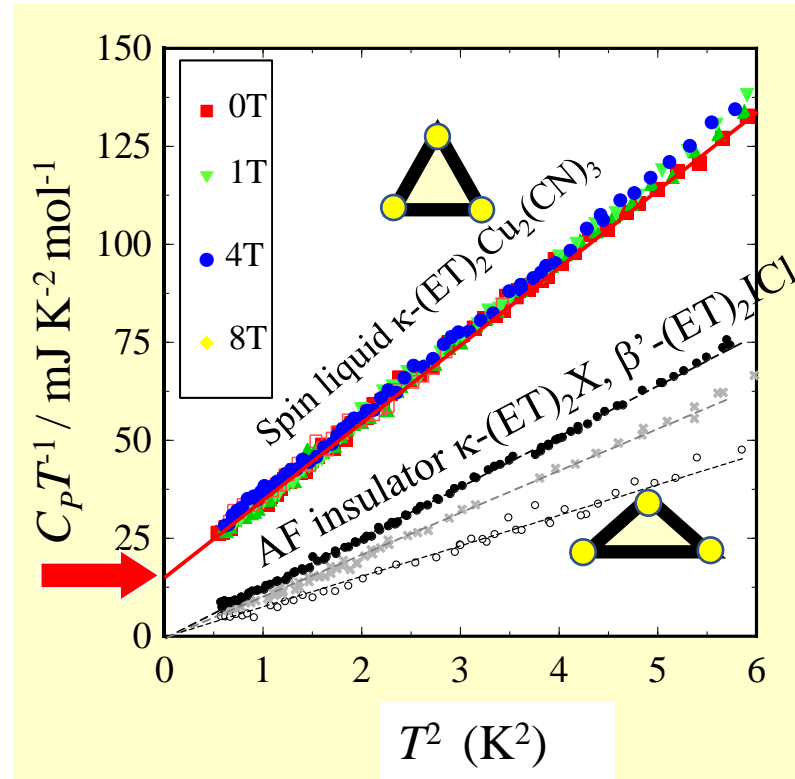


AFM

Shimizu et al., Phys. Rev. Lett. (2003)

Specific heat

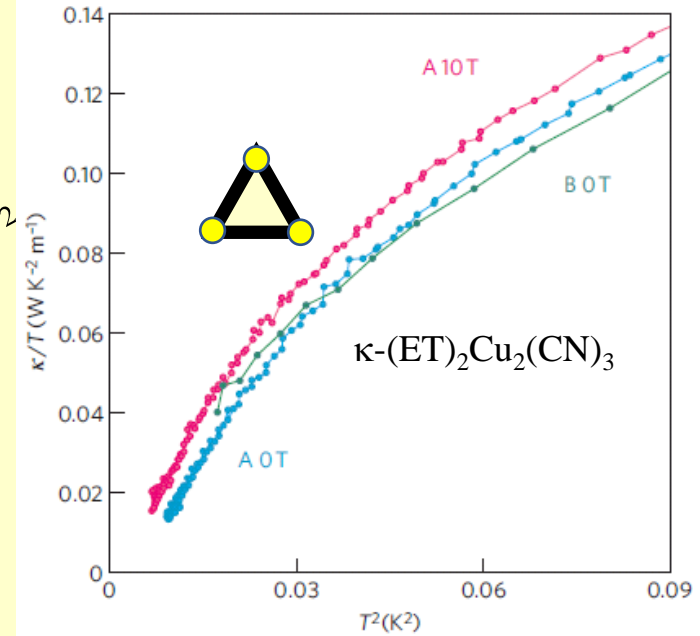
Gapless: $\gamma = 13 \text{ mJ/K}^2\text{mol}$



S. Yamashita *et al.*,
Nat. Phys. 4 (2008) 459

Thermal conductivity

gapped: $\Delta = 0.46 \text{ K}$

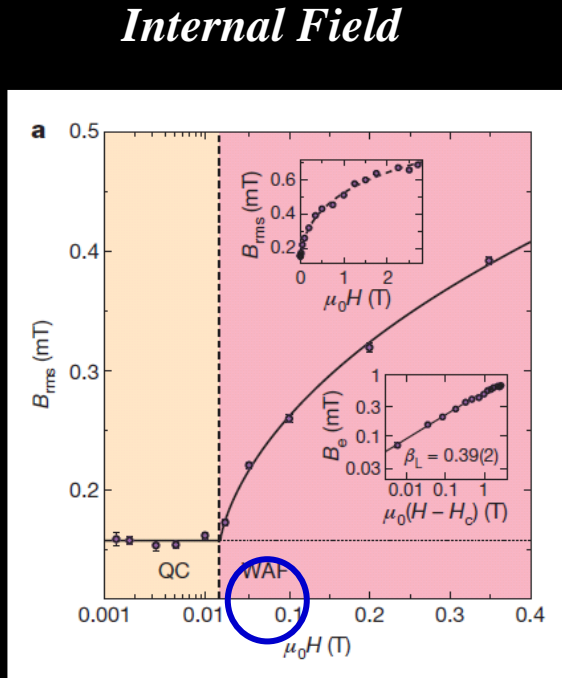


M. Yamashita *et al.*,
Nat. Phys. 5 (2009) 44

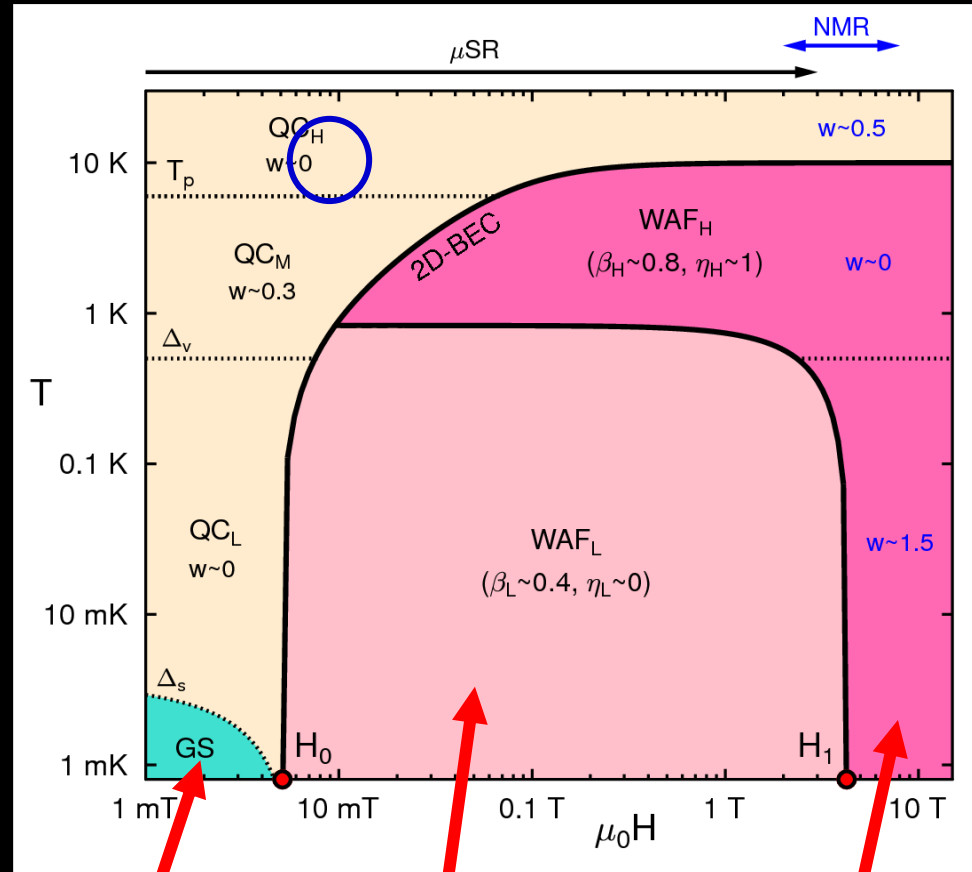
H-T phase diagram determined by μ SR

Pratt et al. *Nature* **471** (2011)612

Inhomogeneous internal field induced by external field



$T = 120$ mK

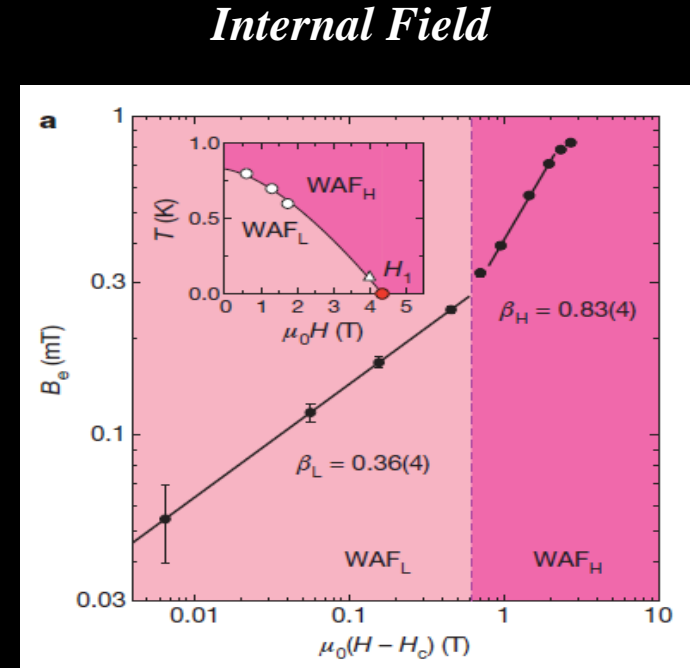


Spin gapped (4 mK)

BEC of Bosonic spinons?
cf. $\text{BaCuSi}_2\text{O}_6$

Deconfined Spinons?
Fermionic?

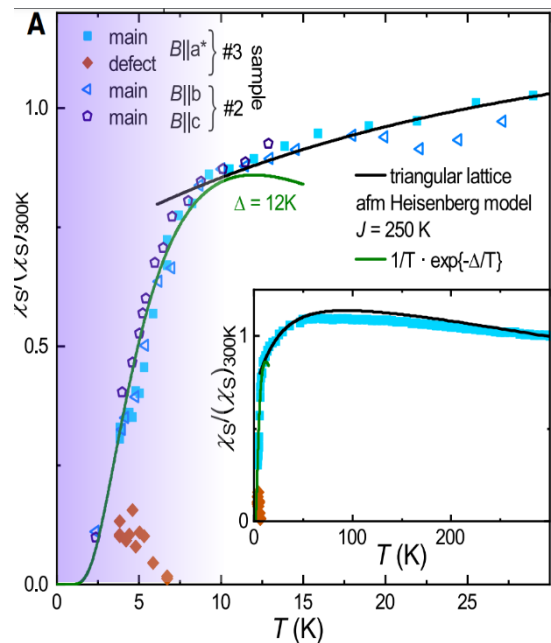
Bosonic spinons
Qi, Xu, Sachdev PRL102(2009)176401



Spin gapped or not at low temperatures ? ESR and NMR

EPR

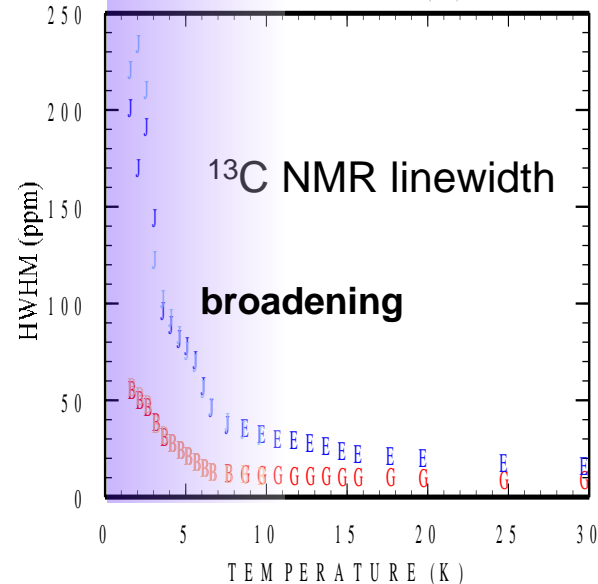
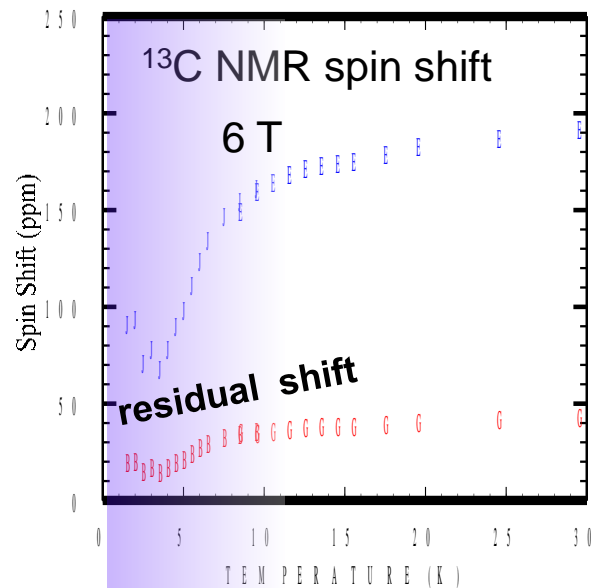
Paramagnetic spins die



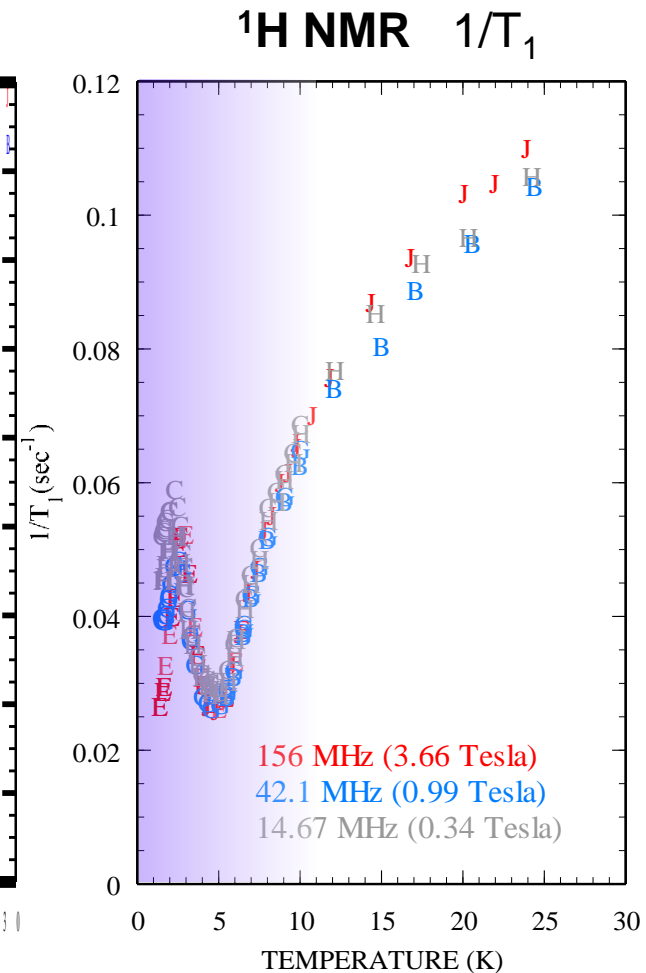
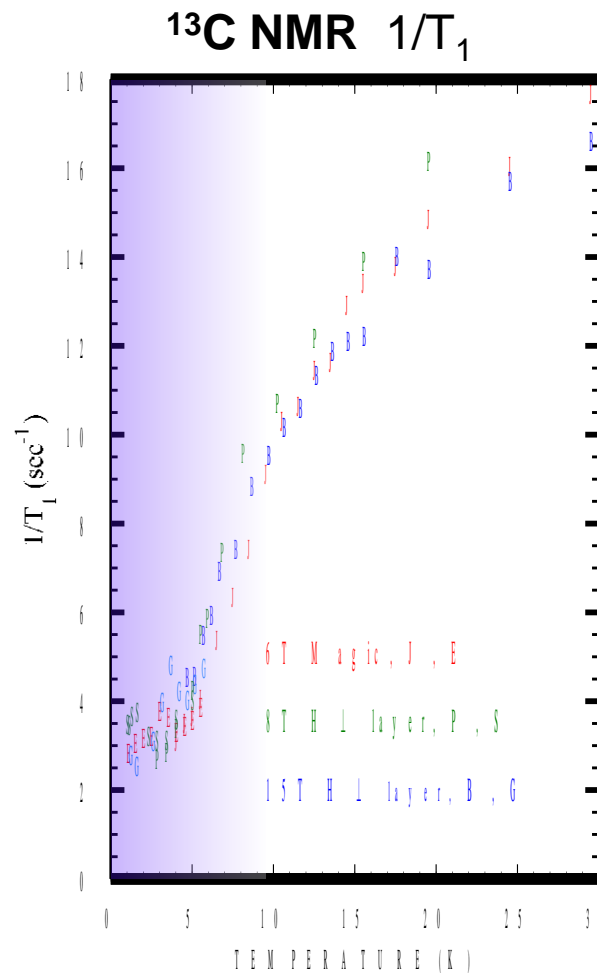
Miksch et al. Science 372, 276 (2021)

$\Delta \sim 10$ K

NMR spectra



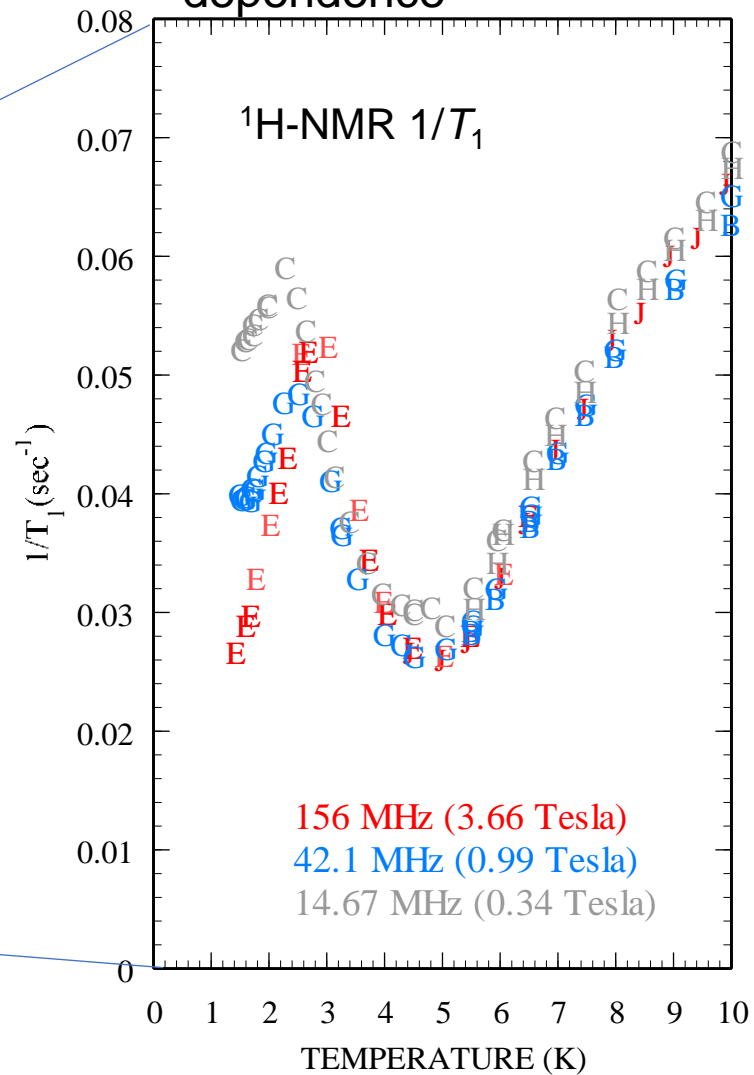
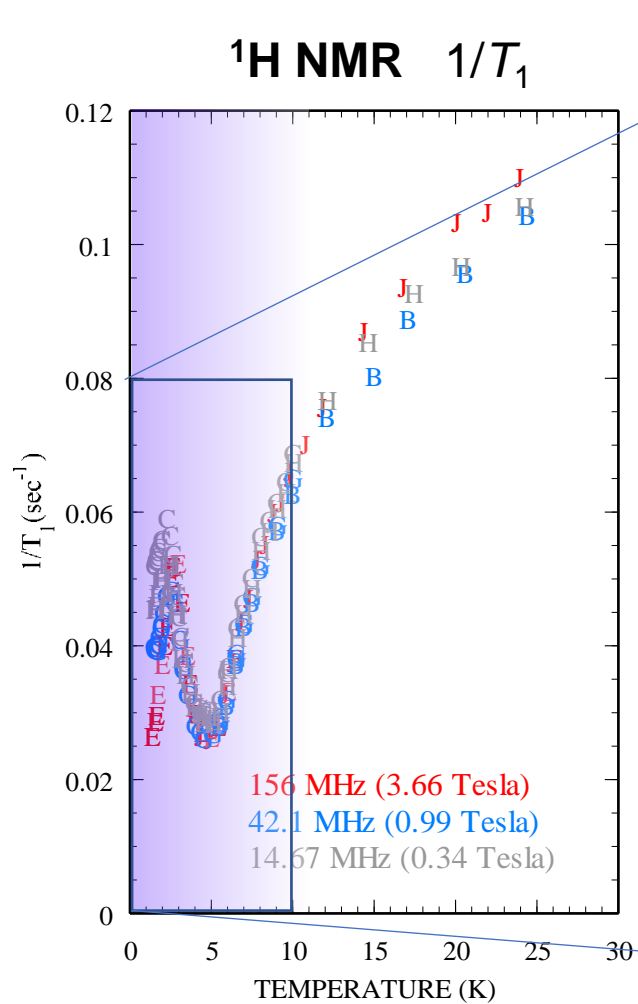
NMR relaxation rate



^1H NMR relaxation rate

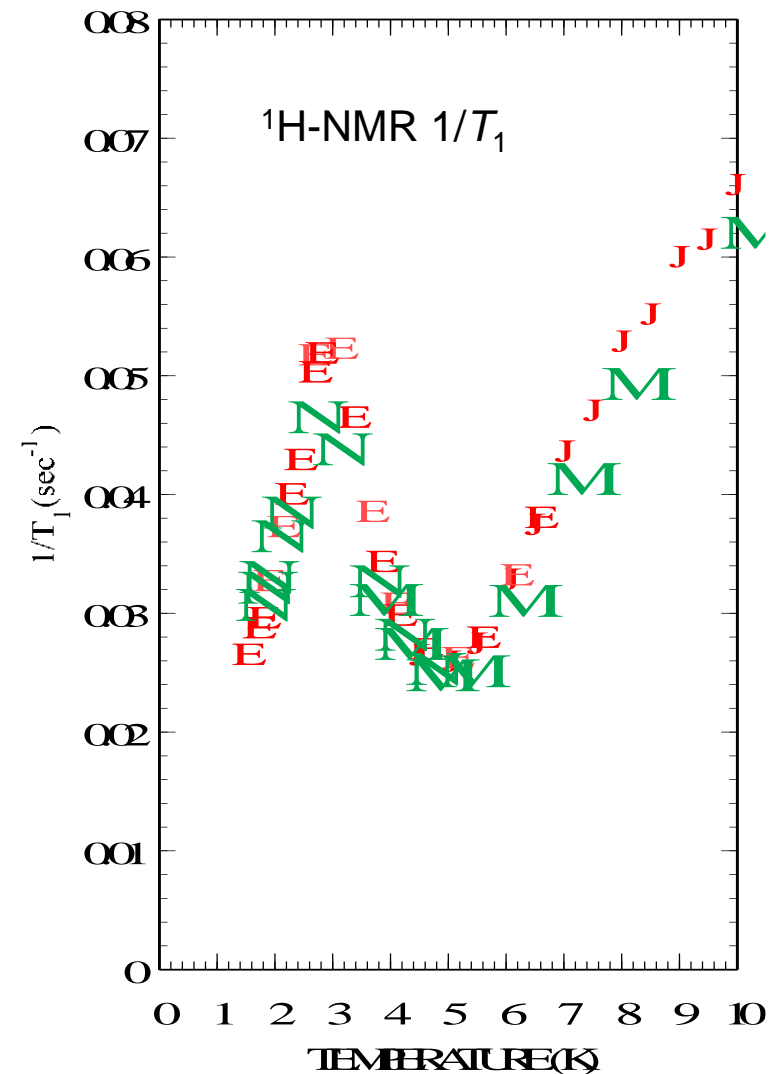


Magnetic field (frequency)
dependence



Field-insensitive above 5 K

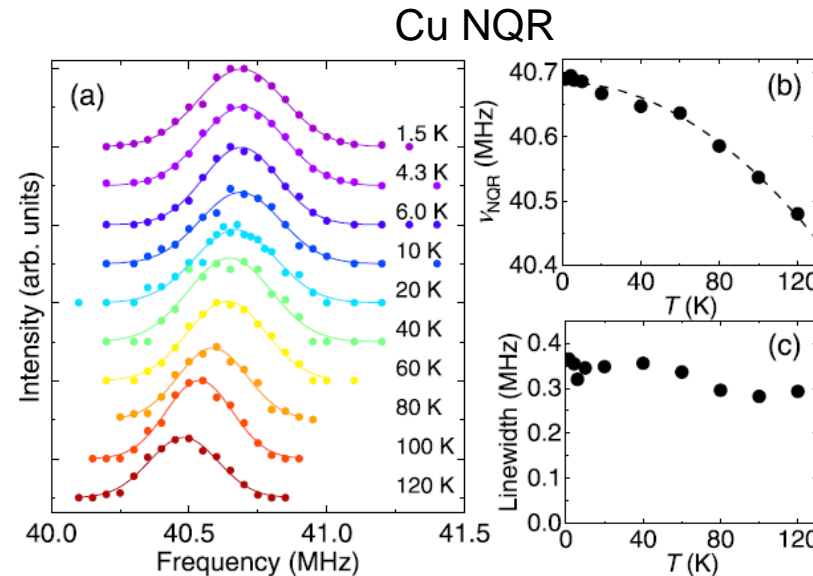
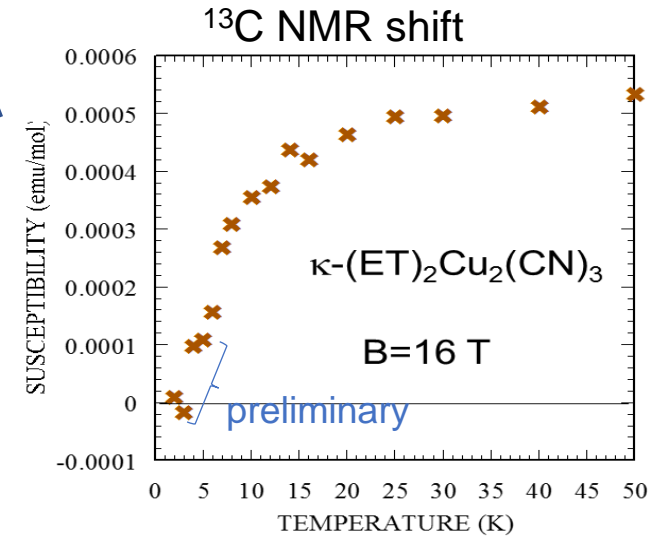
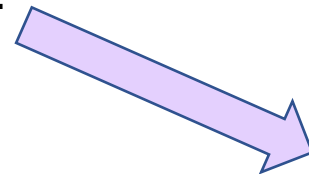
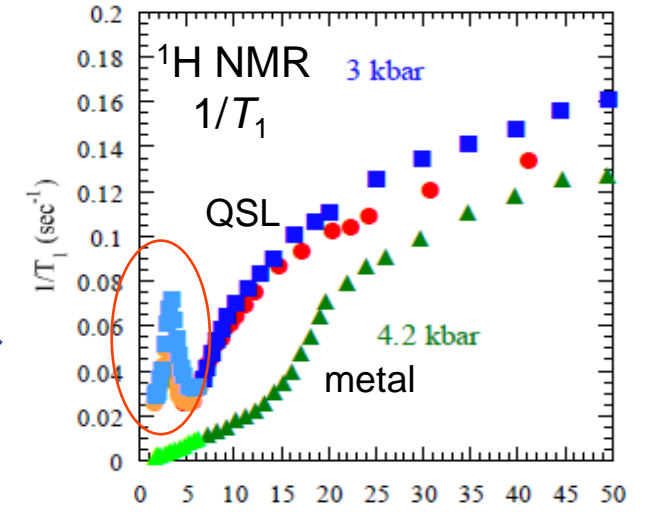
Nearly reproducible
in separate samples



Unconventional spin gapped state: instability of QSL ?

1. Knight shift and $1/T_1$ do not vanish at low-T and line is broadened.
2. $1/T_1$ forms a sharp peak after spin gapped.
The peak disappears in the metallic phase.
3. The spin-gapped feature is robust even against 16 T.
4. No change in NQR spectra across 6 K.

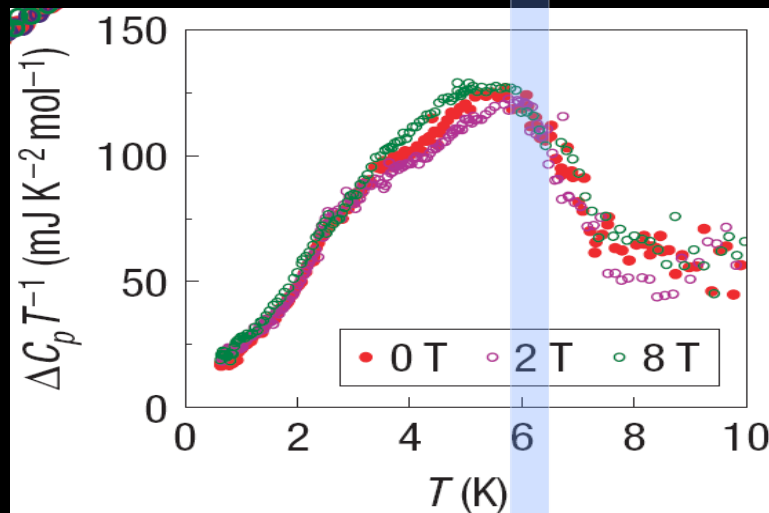
VBC (VBS) ?



6K-anomaly in $\kappa\text{-(ET)}_2\text{Cu}_2(\text{CN})_3$

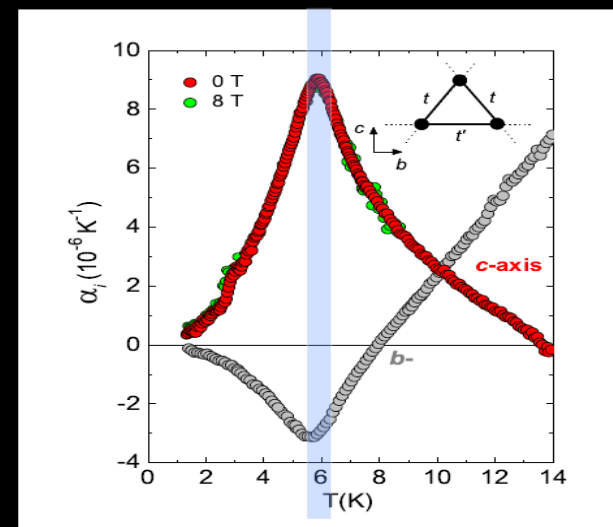
Specific heat

S. Yamashita *et al.*,
Nature Phys. 4 (2008) 459



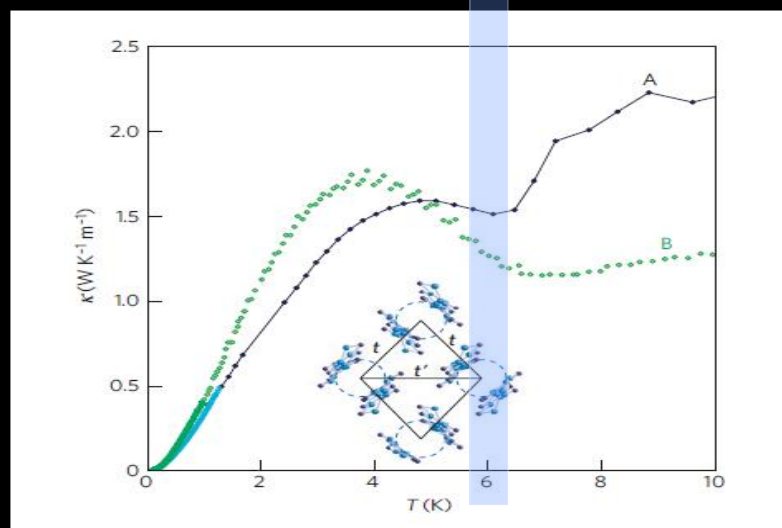
Thermal expansion coefficient

Manna *et al.*, *PRL* 104 (2010) 016403



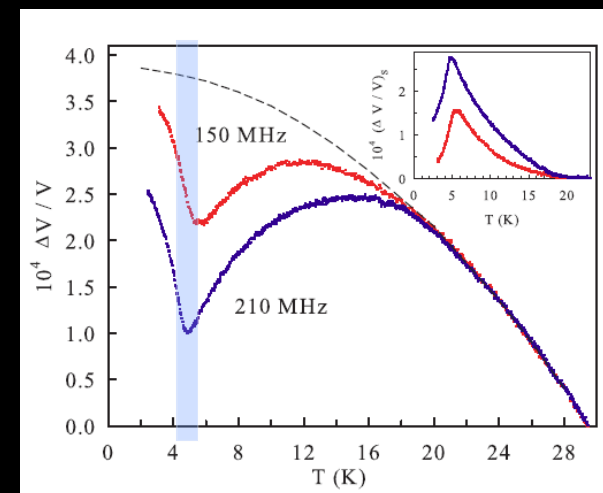
Thermal conductivity

M. Yamashita *et al.*,
Nature Phys. 5 (2009) 44



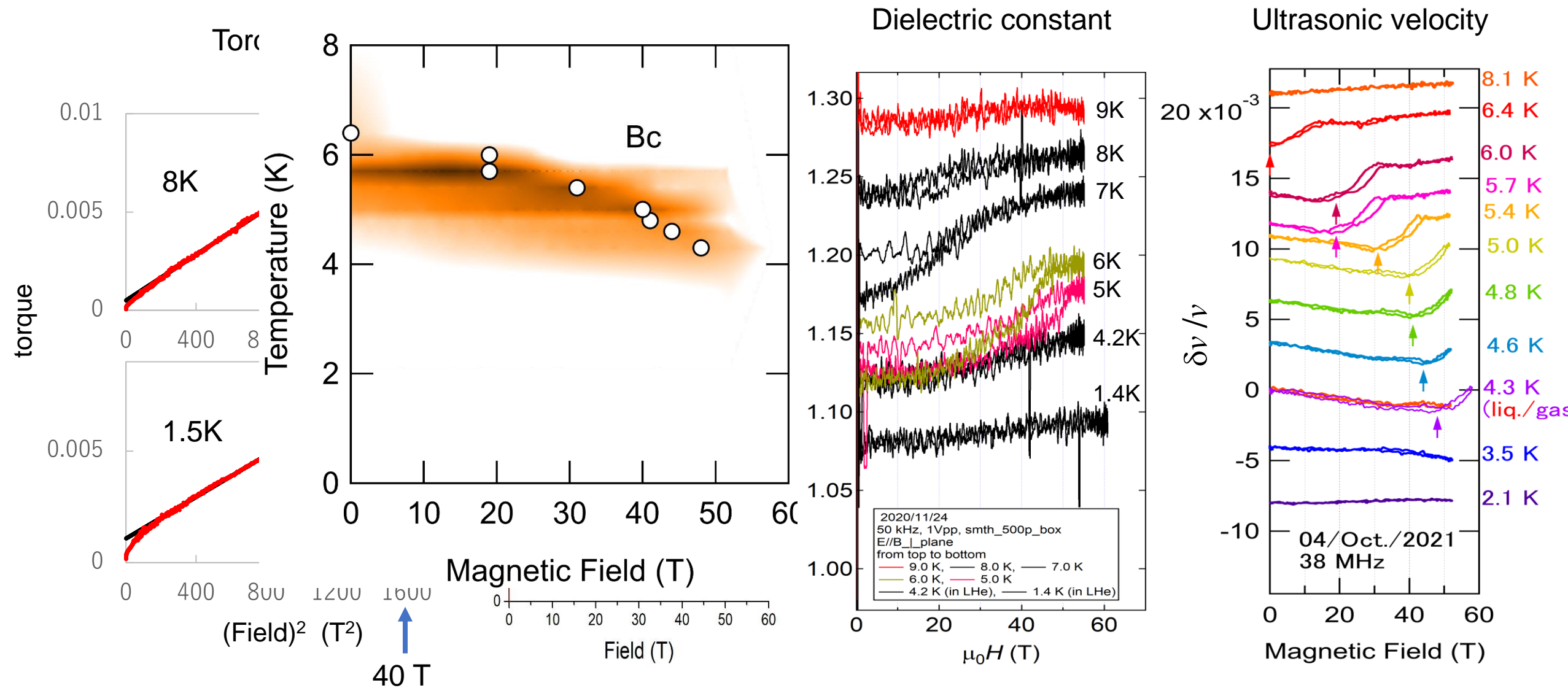
Ultrasound velocity

Poirier *et al.*,



Search for quantum oscillations in κ -(ET)₂Cu₂(CN)₃ with magnetic fields up to 60 Tesla at ISSP

Kohama, Nomura, Miyake, Urai

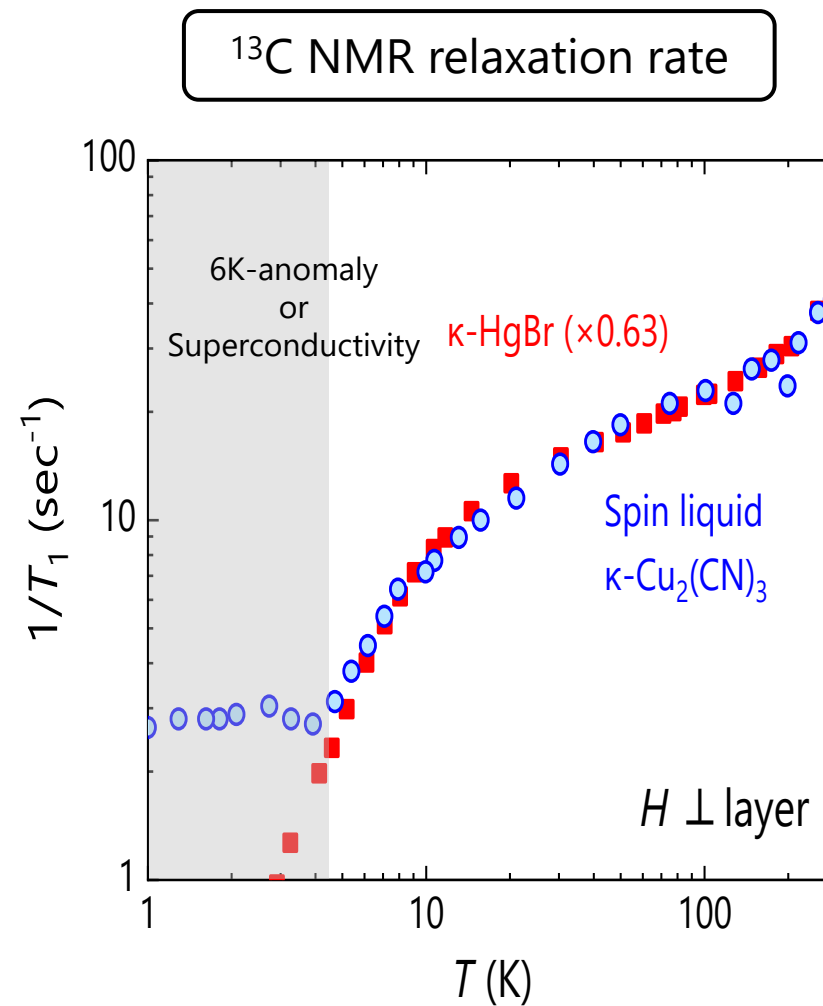
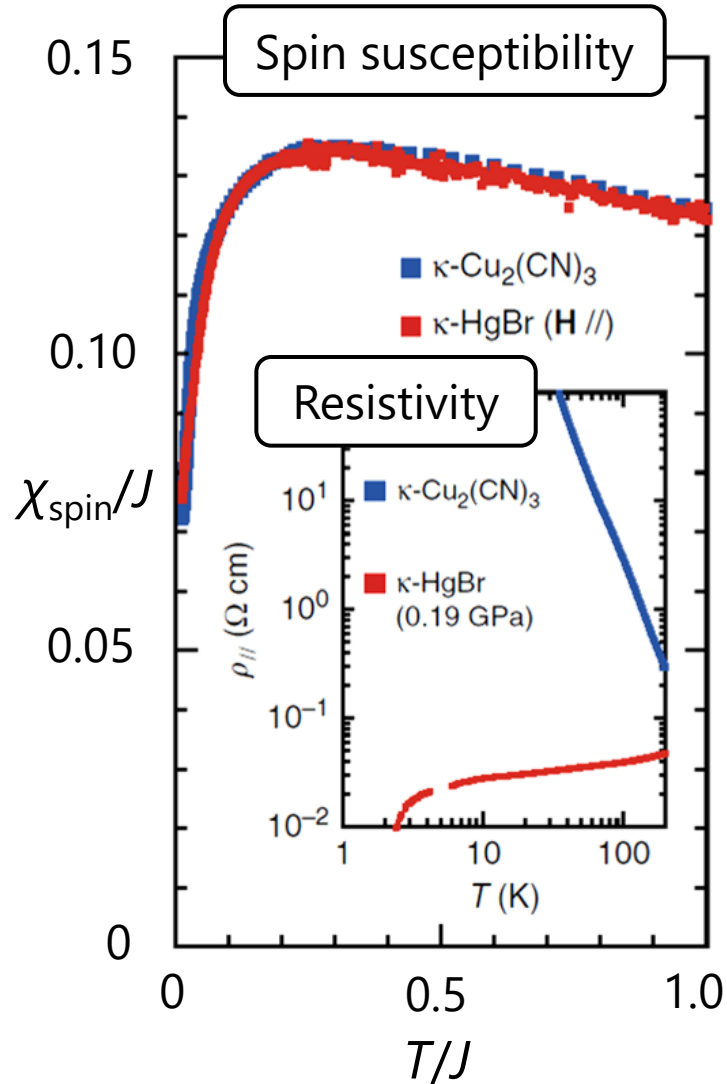


Non-doped and doped QSL candidates

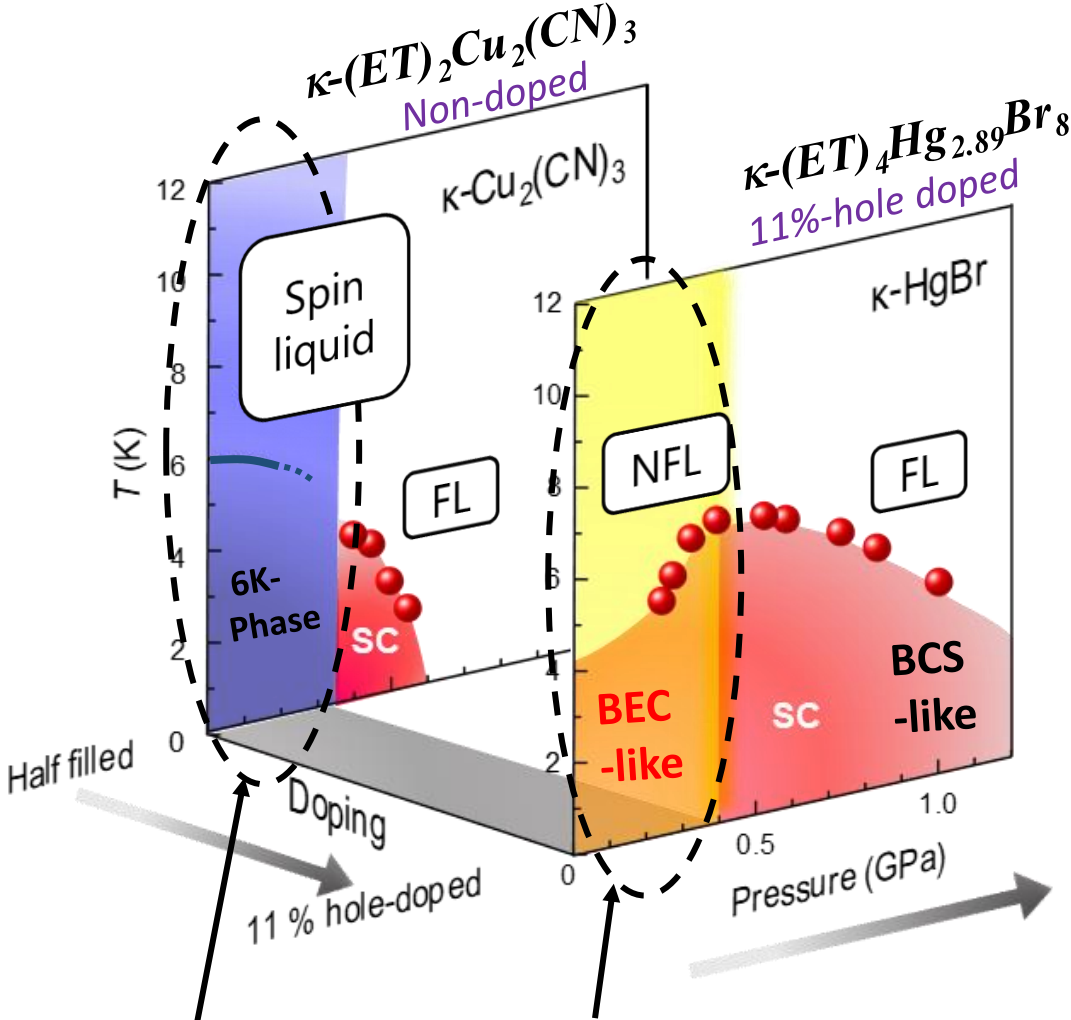
Contrasting conductivity, similar magnetism



Doped QSL



Phase diagram : non-doped and doped spin liquid materials



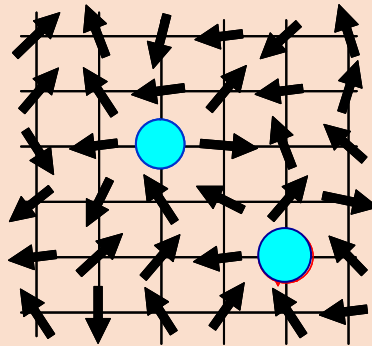
QSL phase	→	non-Fermi liquid
6-K phase	→	superconducting phase

Pressure dependence of Hall coefficient: from doped QSL to correlated metal



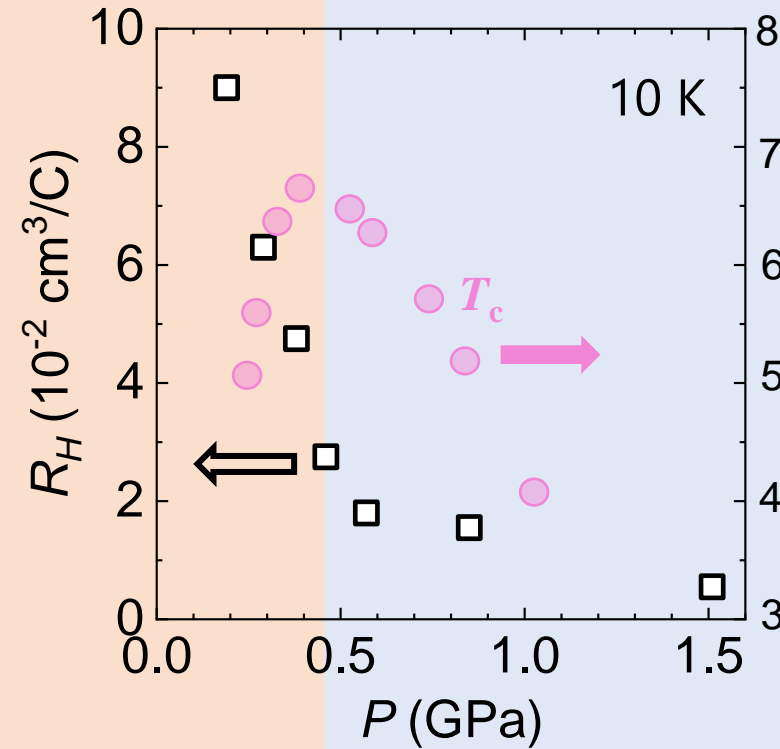
Hall coefficient \sim (*carrier number*)⁻¹

Double occupancy
Prohibited

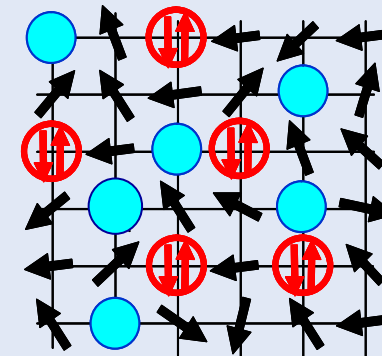


Low carrier density

Doped Mott



Double occupancy
Allowed

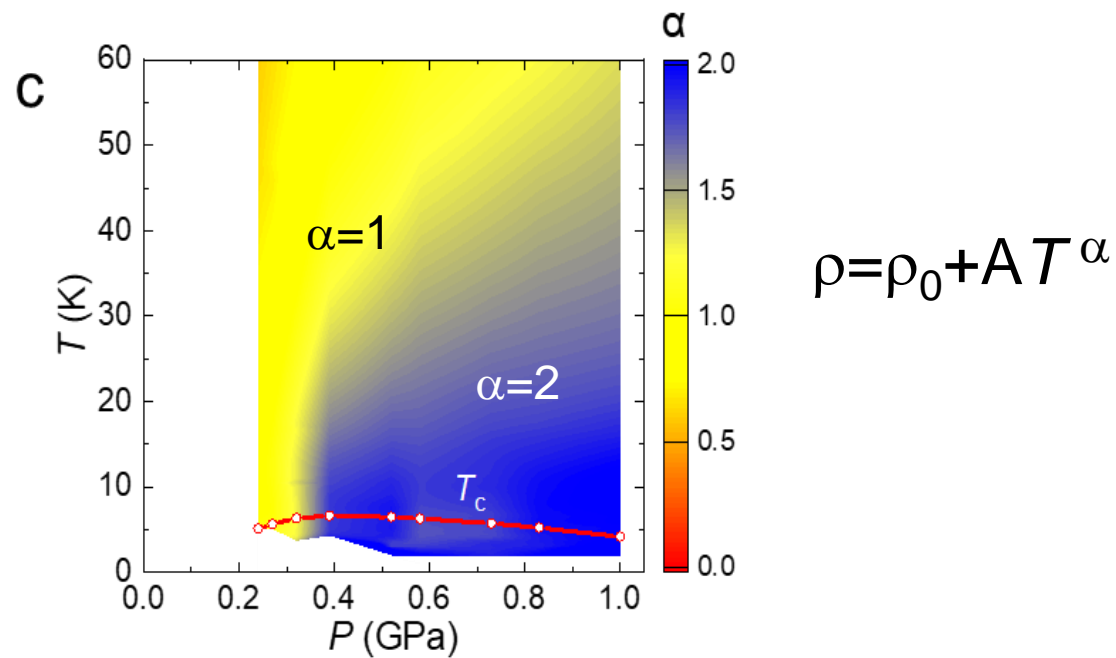
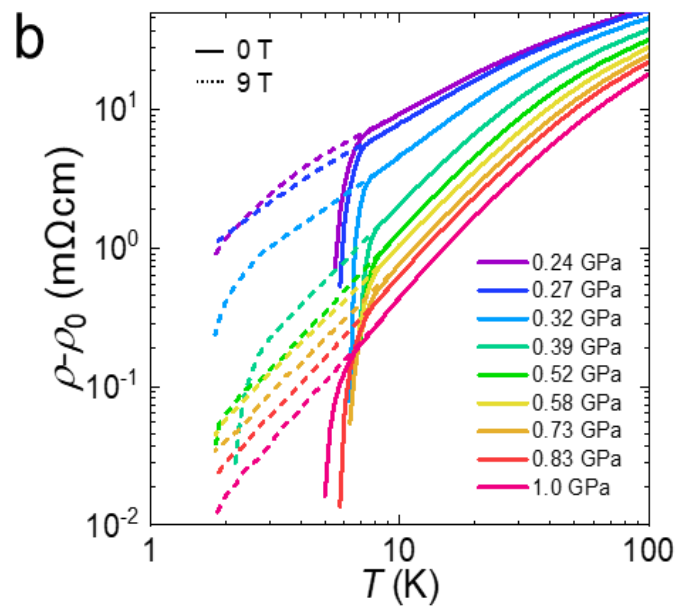
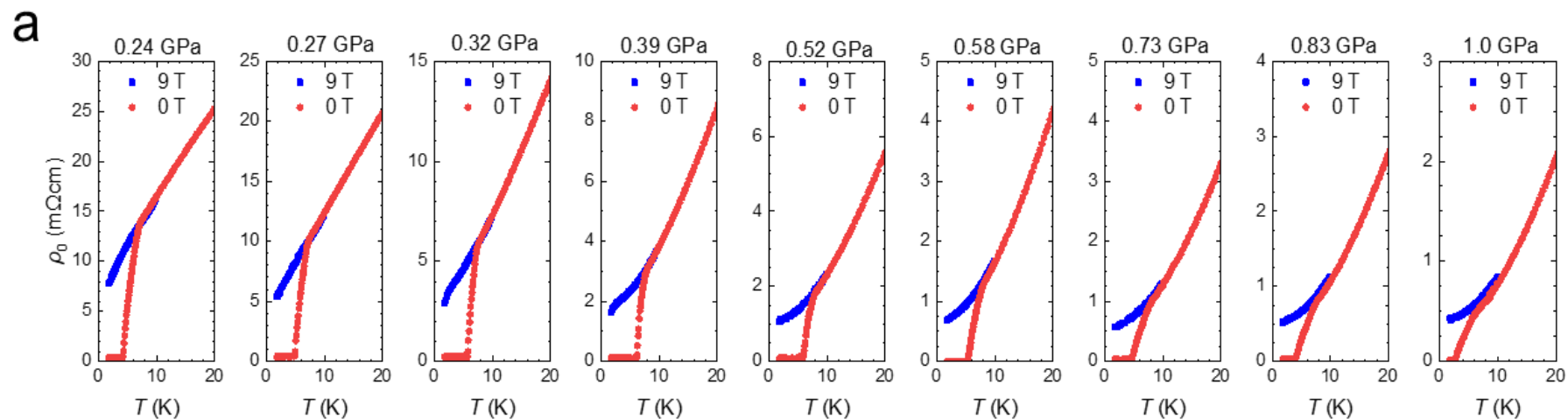


High carrier density

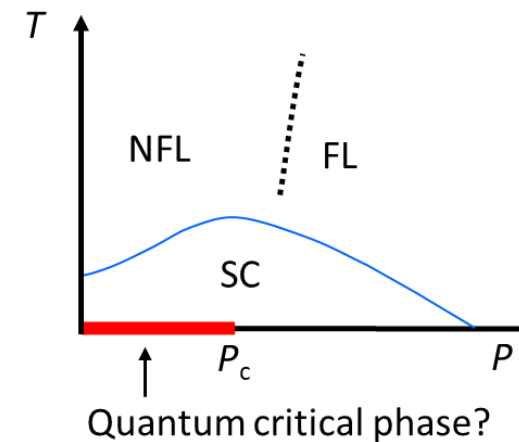
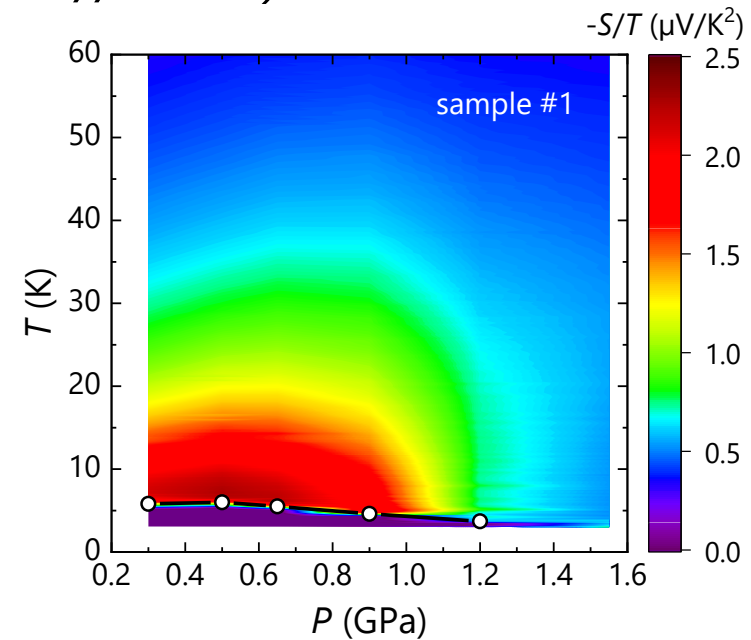
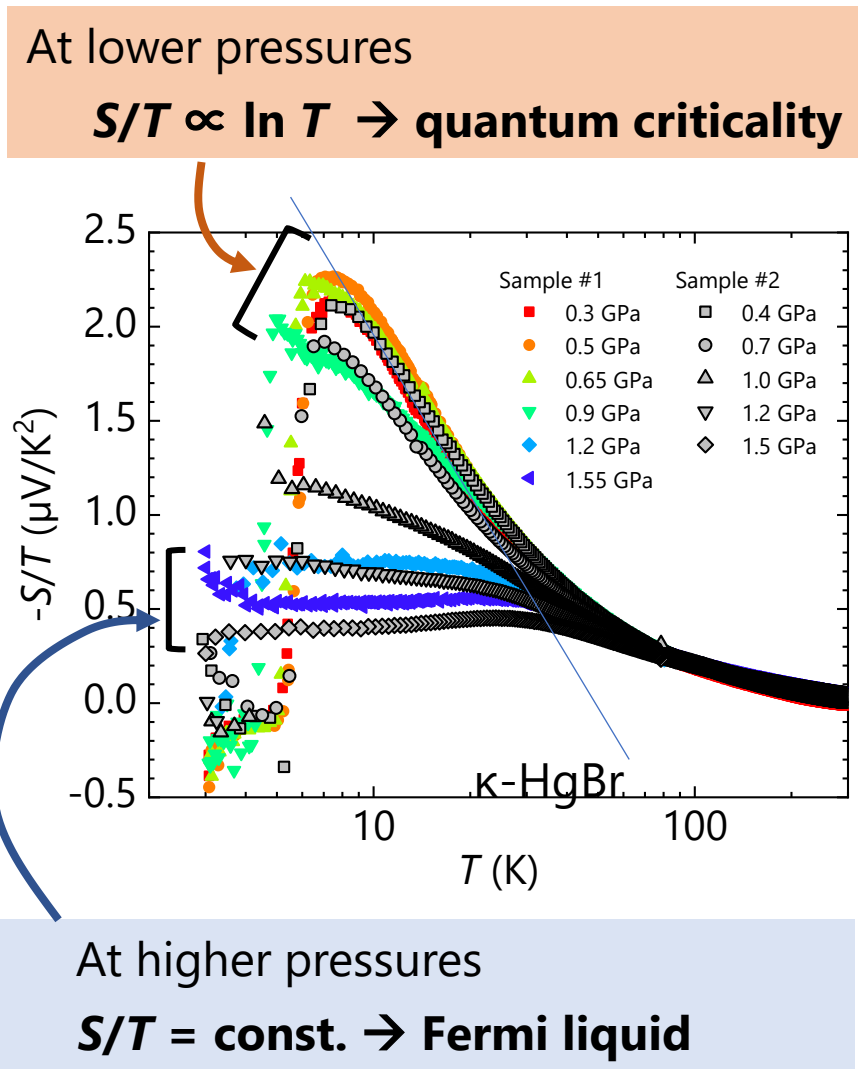
Correlated metal

Non-Fermi liquid to Fermi liquid crossover

$\kappa\text{-(ET)}_4\text{Hg}_{2.89}\text{Br}_8$



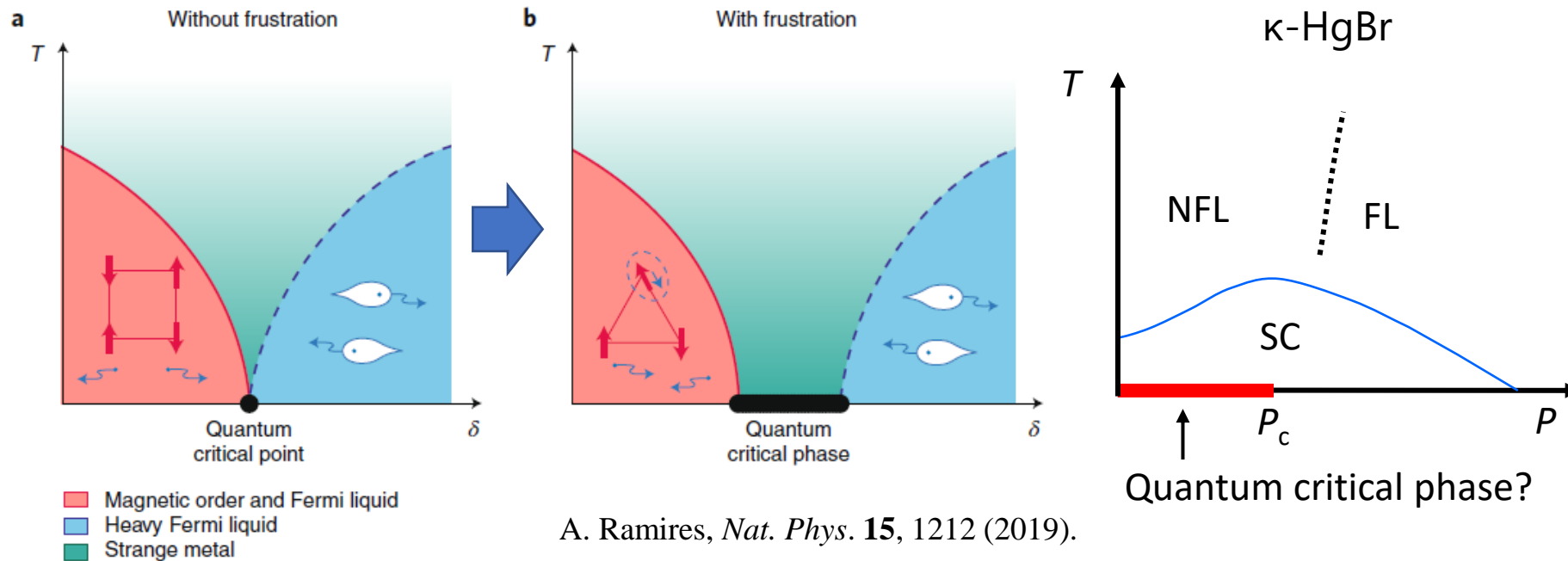
Seebeck coefficient S ($\nabla T // c\text{-axis}$)



Quantum critical "phase"

CePdAl (Heavy fermion system with Kagome lattice)
→ Emergence of quantum critical *phase*, (not a point)
H. Zhao, *et al.*, *Nat. Phys.* **15**, 1261 (2019).

Frustration makes QC point to QC phase



A. Ramires, *Nat. Phys.* **15**, 1212 (2019).

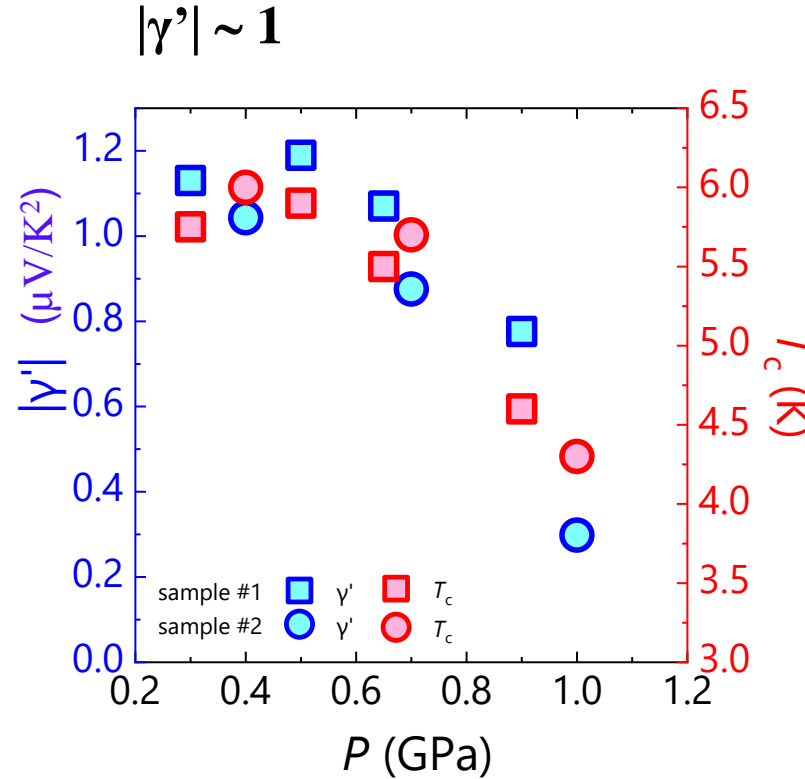
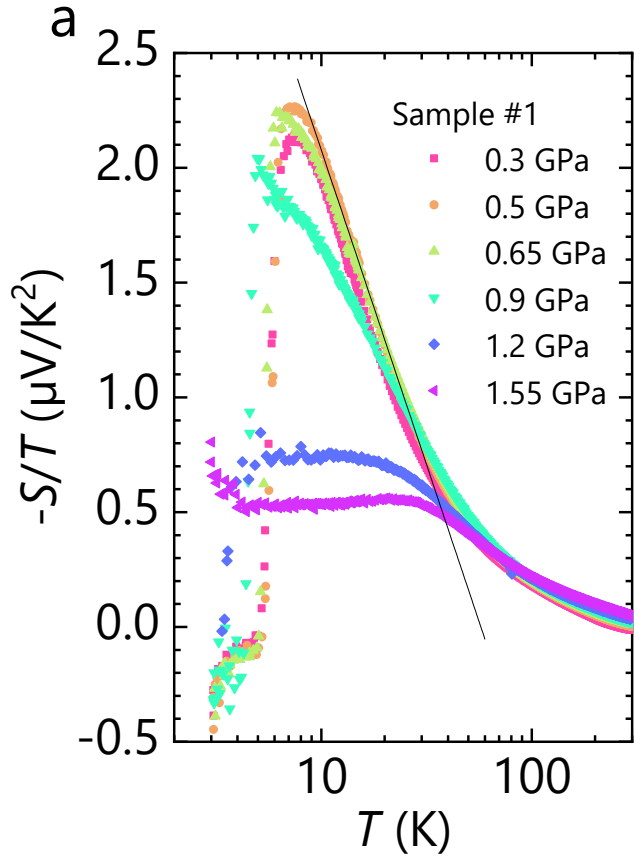
M. Vojta, *Rep. Prog. Phys.* **81**, 064501 (2018)

Strength of Quantum criticality



Table S1 | $|\gamma'|$ values in the logarithmic part of $-S/T$
The $|\gamma'|$ values in $S/T = \gamma' \ln(T/T_0)$ in the unit of $\mu\text{V}/\text{K}^2$.

$$S/T = \gamma' \ln(T/T_0) \quad (10 \text{ K} < T < 30 \text{ K})$$



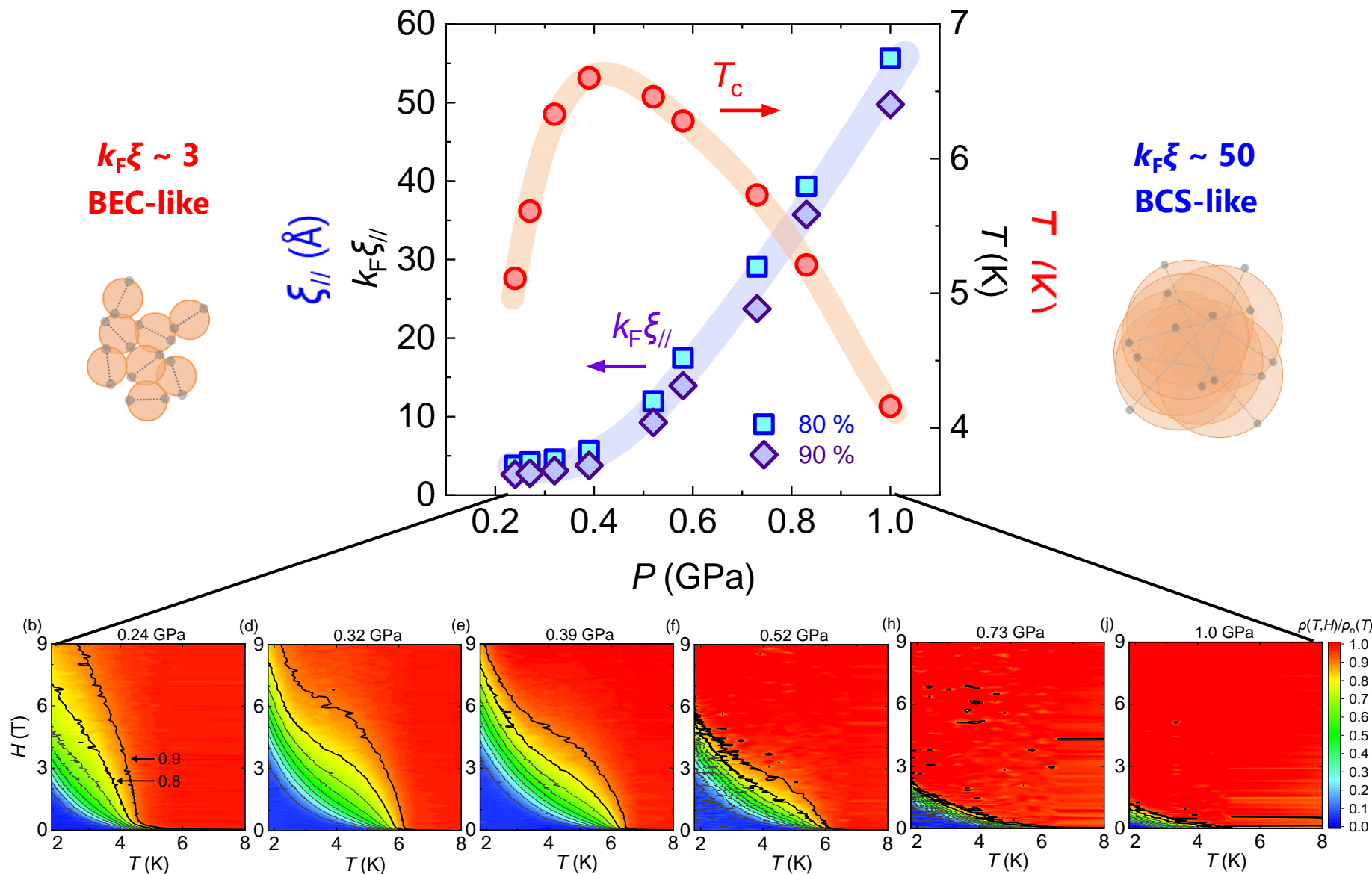
T_c and γ' are scaled to each other

Material	Slope value
Nd-LSCO ($p = 0.24$) (ref. ⁶)	0.11
Eu-LSCO ($p = 0.24$) (ref. ⁷)	0.16
Bi2201 ($p = 0.39$) (ref. ⁸)	0.05
PCCO ($x = 0.16\text{-}0.19$) (ref. ⁹)	0.012-0.038
LCCO ($x = 0.15\text{-}0.17$) (ref. ⁹)	0.0095 – 0.049
[BiBa _{0.66} K _{0.36} O ₂]CoO ₂ (ref. ¹⁰)	0.62
Ba(Fe _{1-x} Co _x) ₂ As ₂ ($p=0.022\text{-}0.13$) (ref. ¹¹)	0.32 - 0.895
EuFe ₂ (As _{1-y} P _y) ₂ ($y=0.26, 0.36$) (ref. ¹⁸)	0.077, 0.16
UCoGe (H=11.1 T) (ref. ¹²)	2.3
YbRh ₂ Si ₂ (ref. ¹³)	4.5
CeCu _{5.9} Au _{0.1} (ref. ¹⁴)	6.2
Ce ₂ PdIn ₈ (ref. ¹⁵)	1.6
YbAgGe (ref. ¹⁶)	4.7
YbPtBi (ref. ¹⁷)	0.25

Pressure-induced BEC to BCS

$\kappa\text{-(ET)}_4\text{Hg}_{2.89}\text{Br}_8$

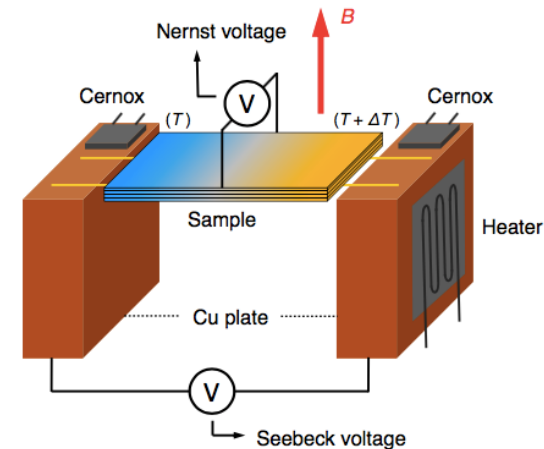
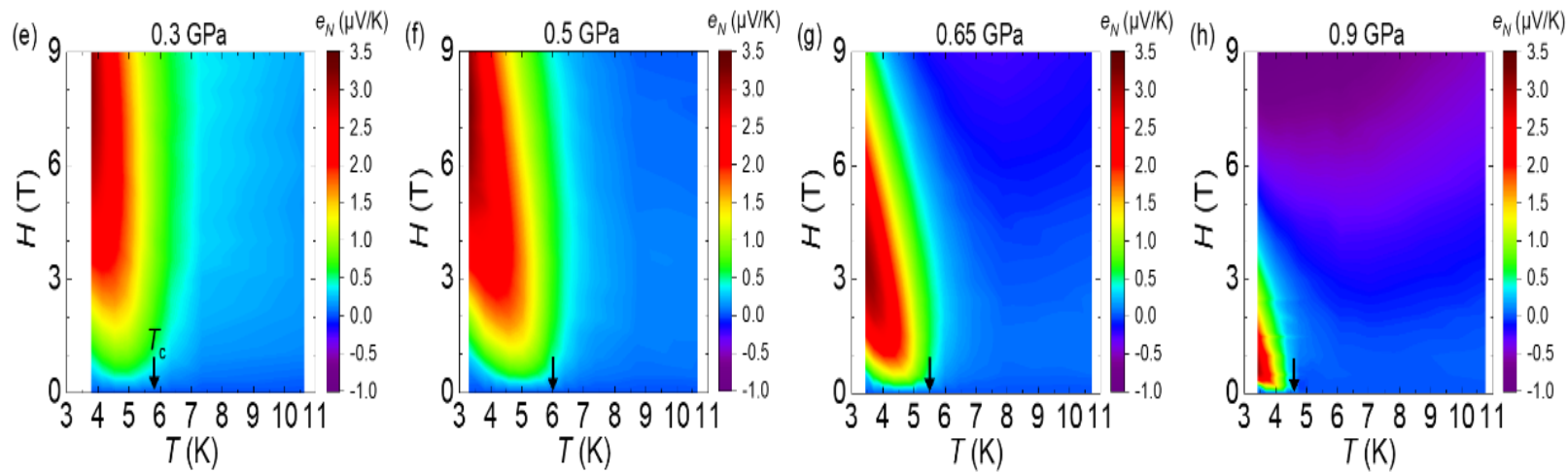
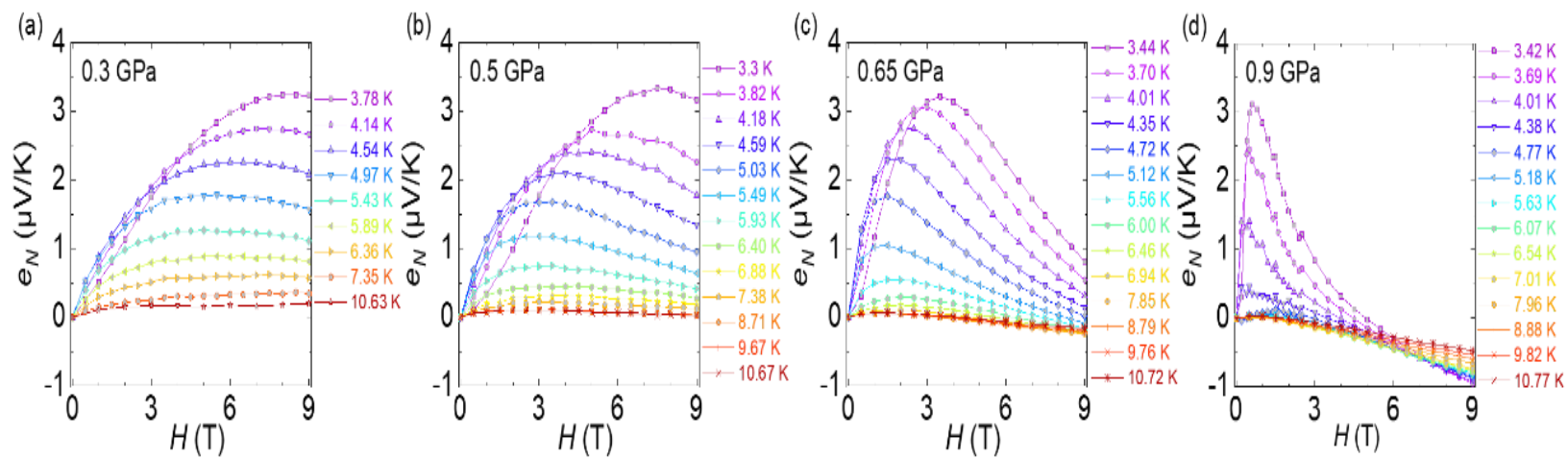
Y. Suzuki *et al.*, Phys. Rev. X **12**, 011016 (2022).



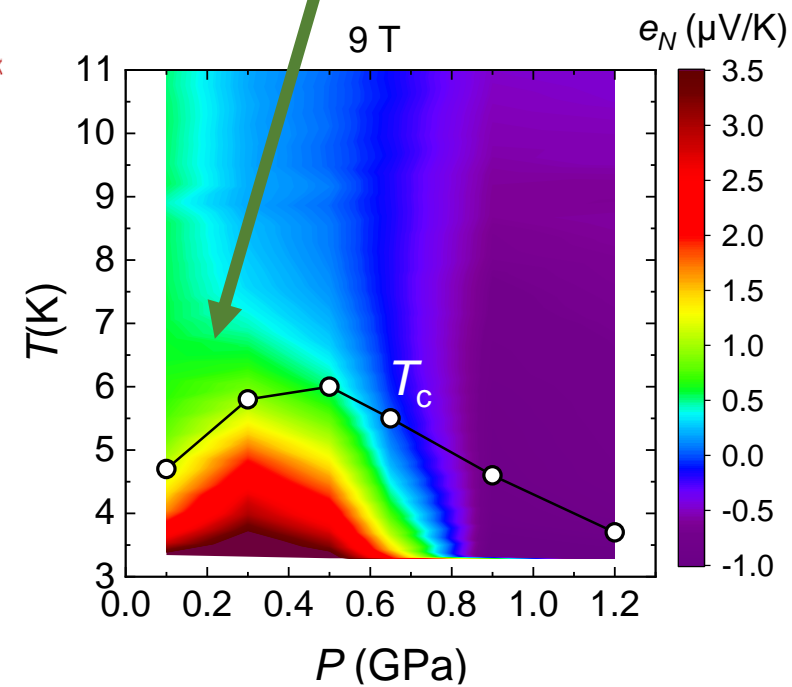
Nernst effect



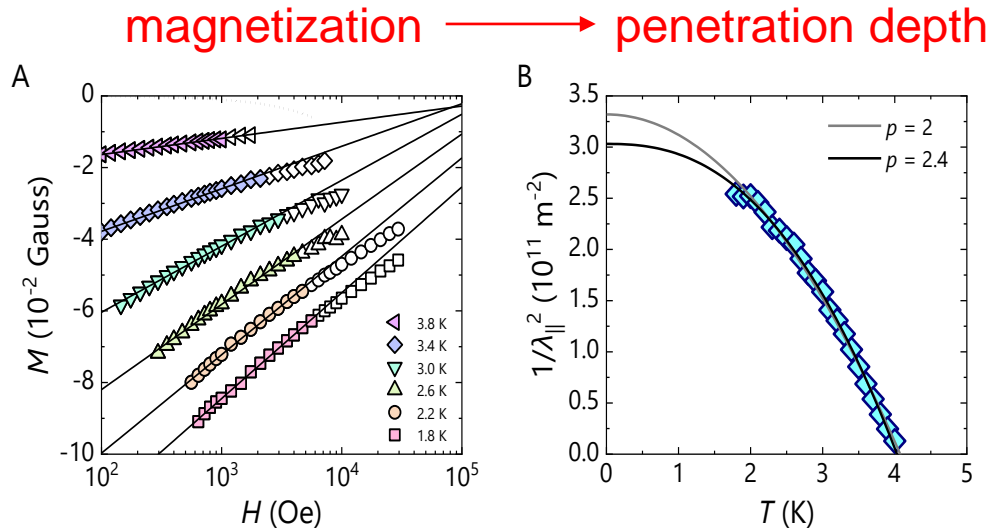
Field-robust superconductivity



Preformed pairs



Superfluid density

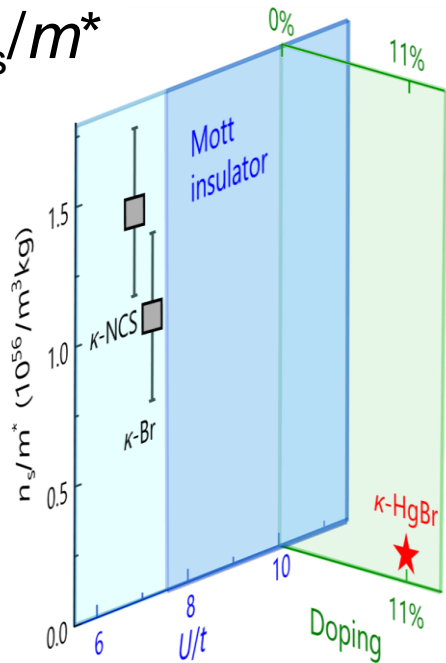


$$-4\pi M = \frac{\varphi_0}{8\pi\lambda^2} \ln\left(\frac{\beta H_{c2}}{H}\right)$$

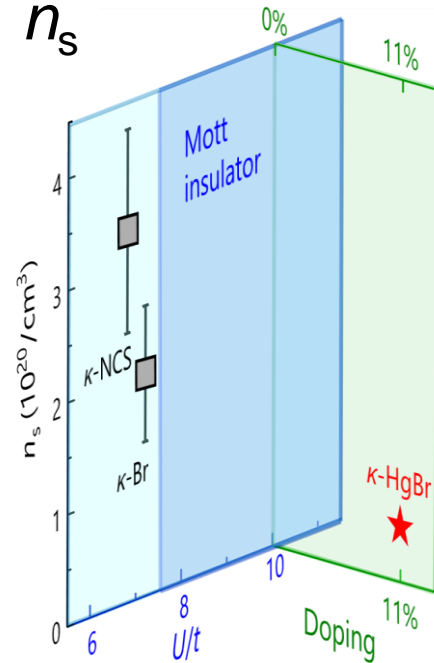
cf. M. Lang et al., *Phys. Rev. B* **46**, 5822-5825 (1992).

$$\frac{n_s}{m^*} = \frac{c^2}{4\pi e^2} \frac{1}{\lambda_L^2}$$

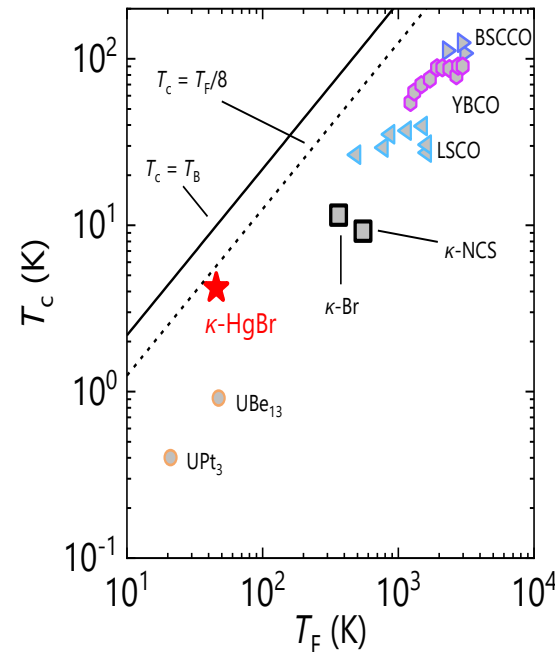
n_s/m^*



n_s



Uemura plot



Reduced superfluid density

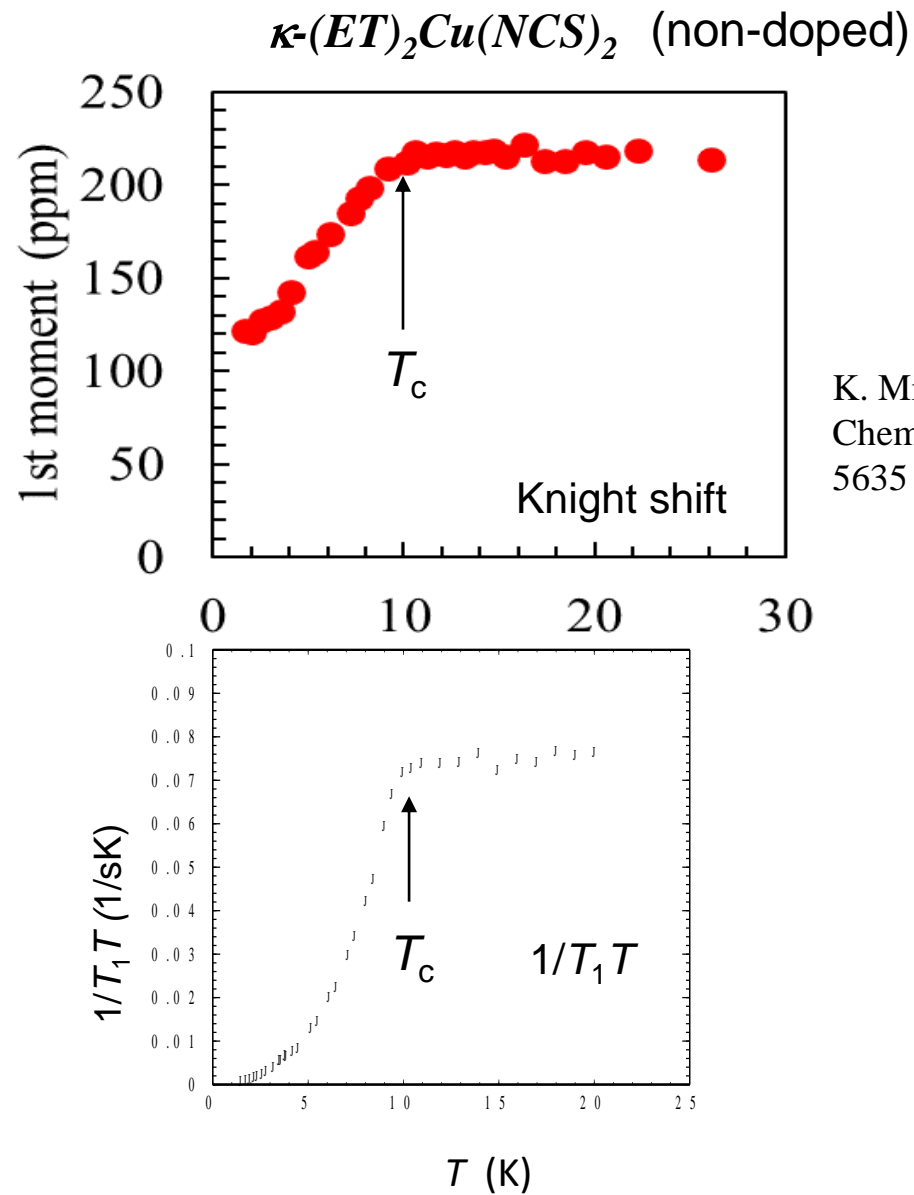
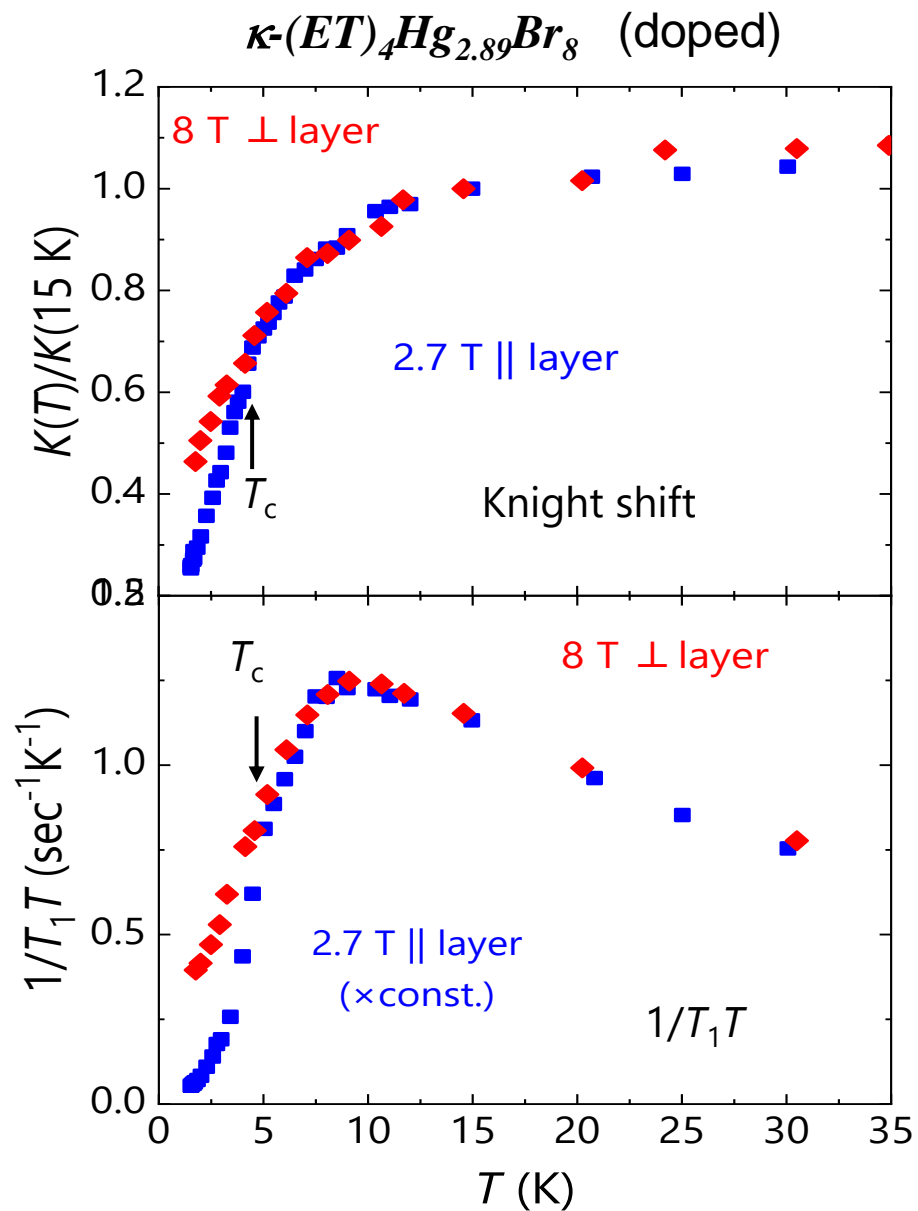
$n_s \sim 15\text{-}25\%$ of total carriers

Large T_c/T_F ratio

$T_c/T_F \sim 0.1$

^{13}C NMR Knight shift and relaxation rate $1/T_1$

Preformed pairs (and pseudo-gapped metal)

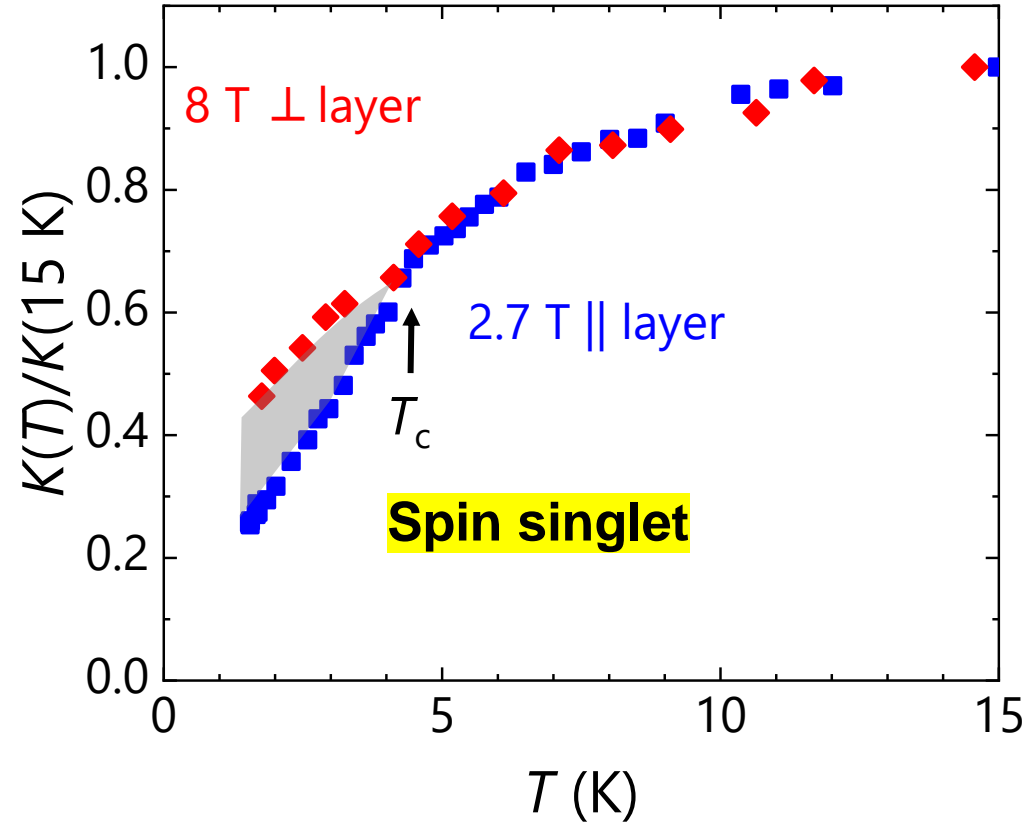


K. Miyagawa *et al.*,
Chem. Rev. **104**,
5635 (2004).

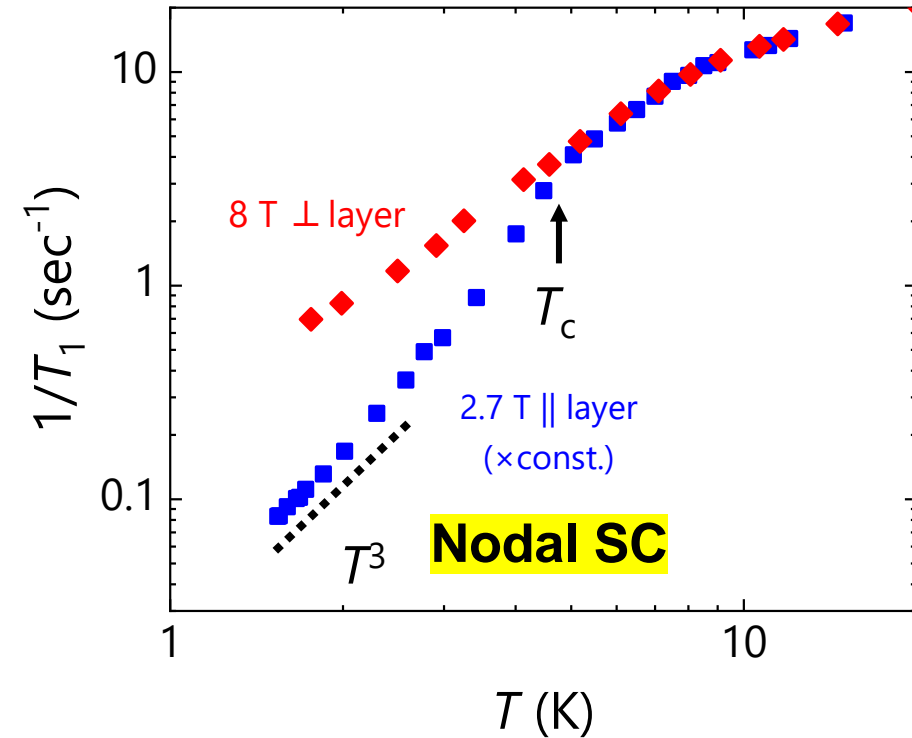
Pairing symmetry: ^{13}C NMR



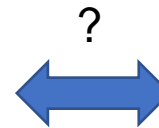
Knight shift



Relaxation rate

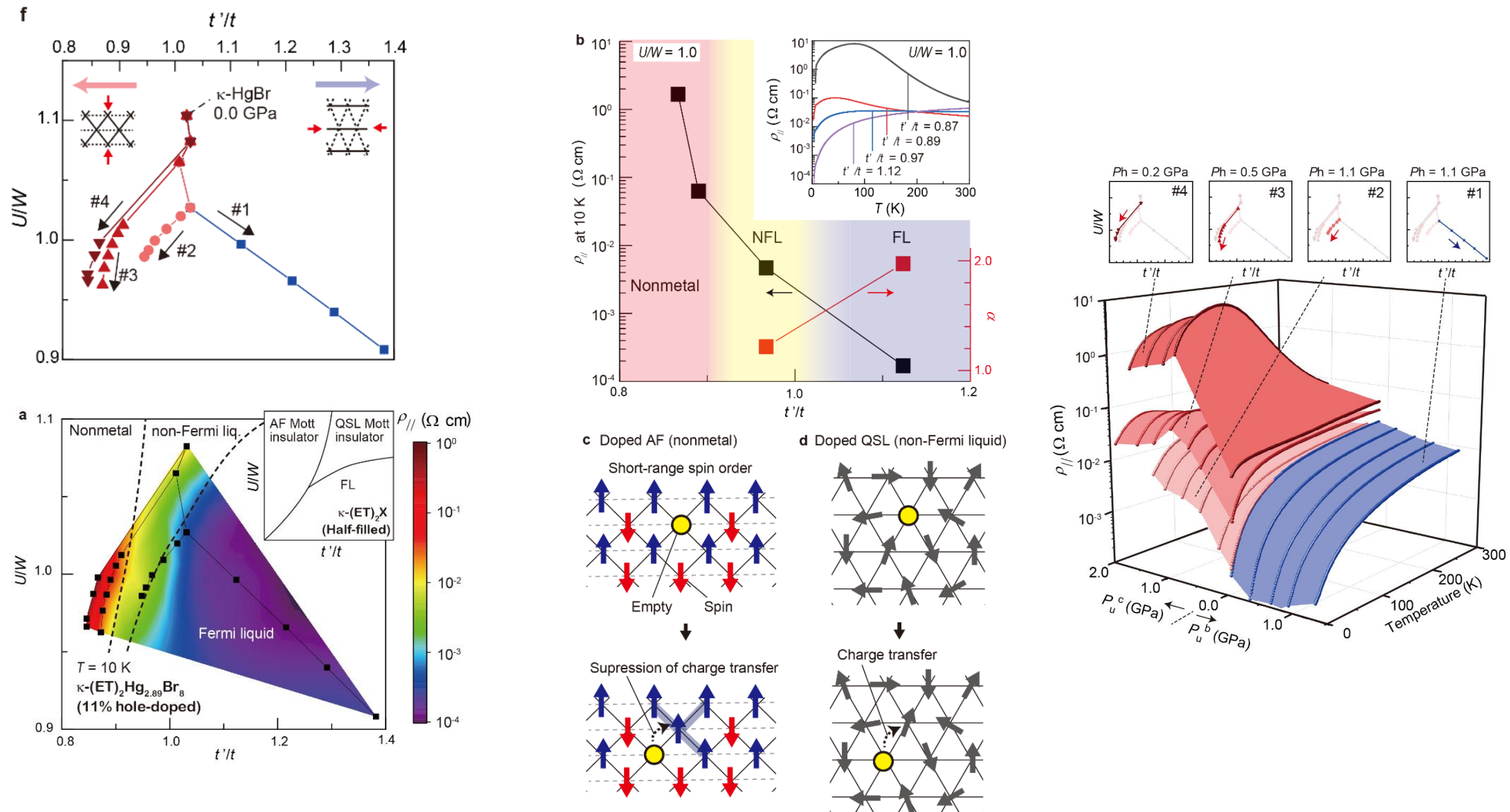


Spin-singlet nodal superconductivity ?



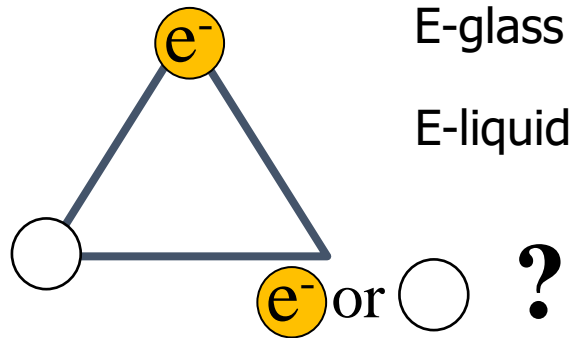
BEC-like pairing

Combination of hydrostatic and uniaxial pressures: variations of U/t and t'/t



Electron (charge) glass

Quarter-filled band electrons
on triangular lattice



Charge frustration

Electronic version of soft matters

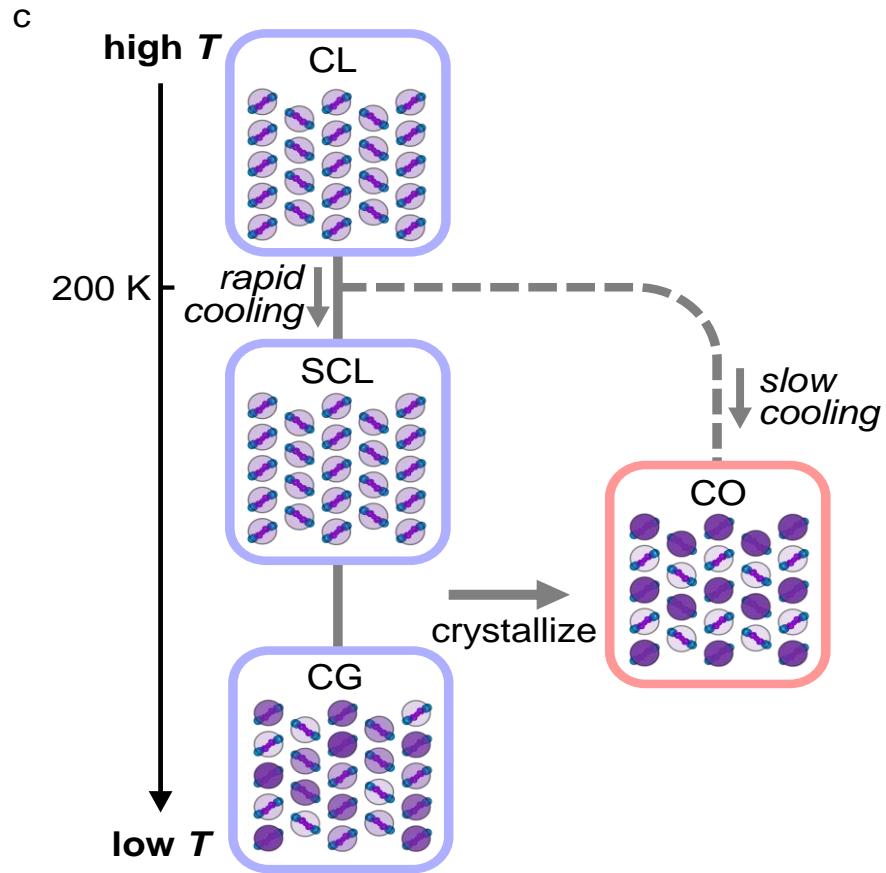
J. Schmalian¹ and P. G. Wolynes, PRL 85, 836 (2000)

Self-Generated Randomness

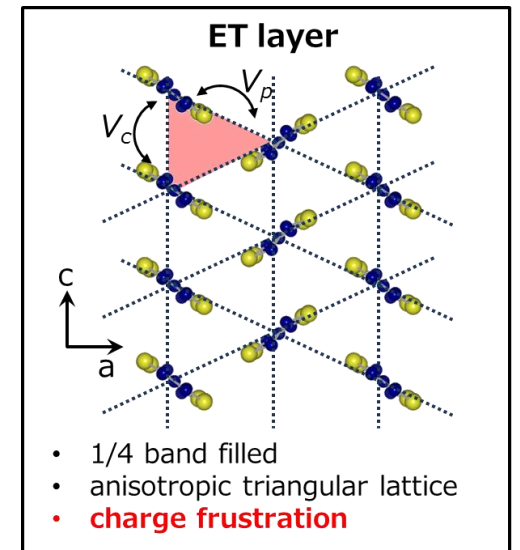
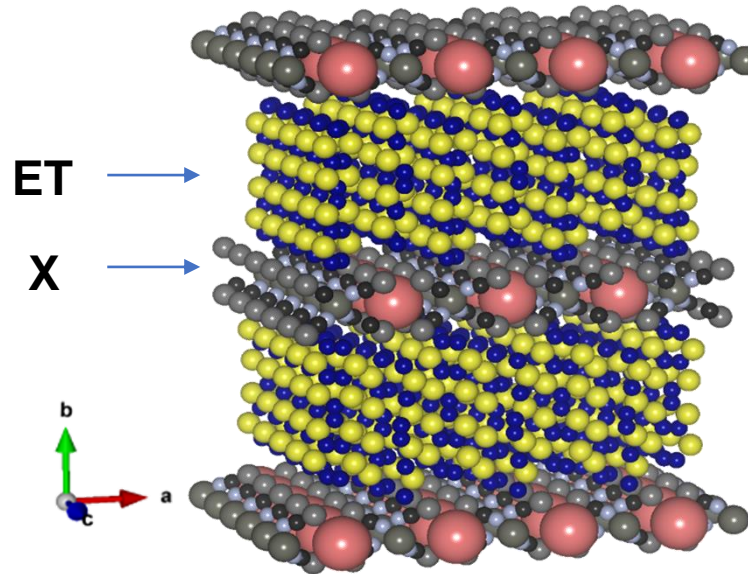
Electronic mayonese

Electron glass

- ✓ Quantum nature
- ✓ Controllable lattice geometry



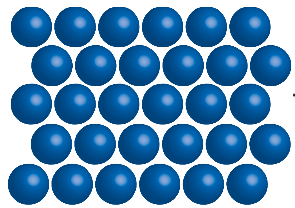
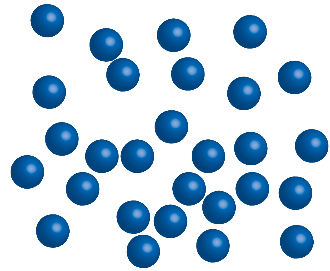
Charge frustrated materials, θ -(ET)₂X



Non-Equilibrium in Supercooled Liquid

Frustration is a key to holding supercooled liquid and glass

Non-equilibrium



Volume

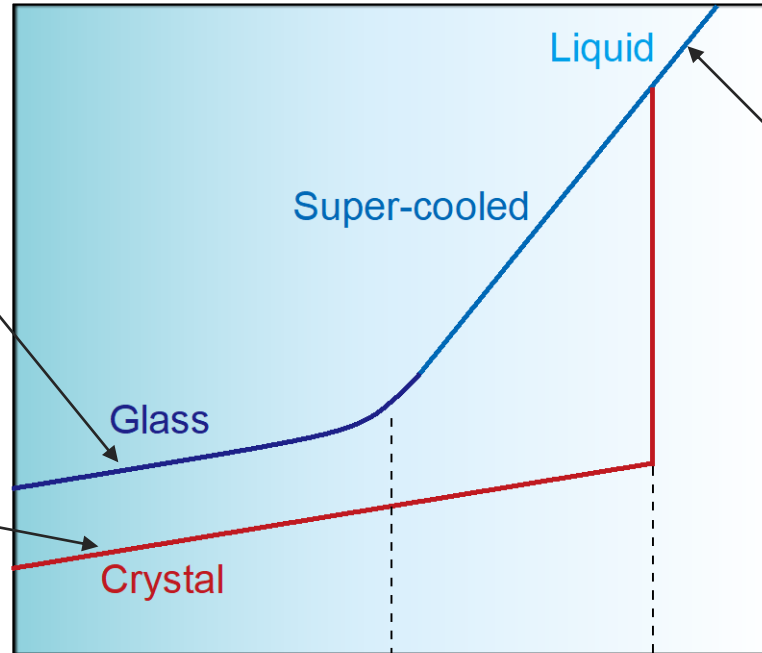
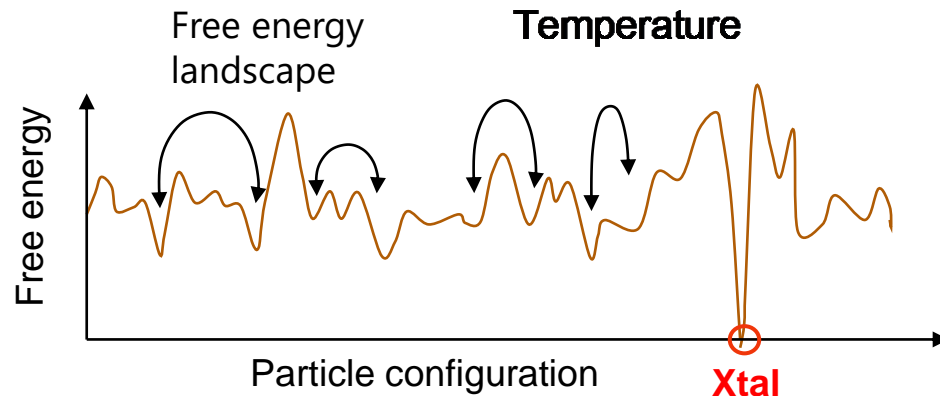
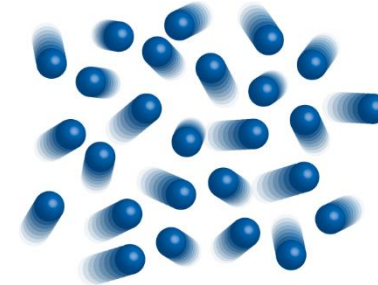


figure from
Dobenedetti & Stillinger
Nature 410, 259 (2001).

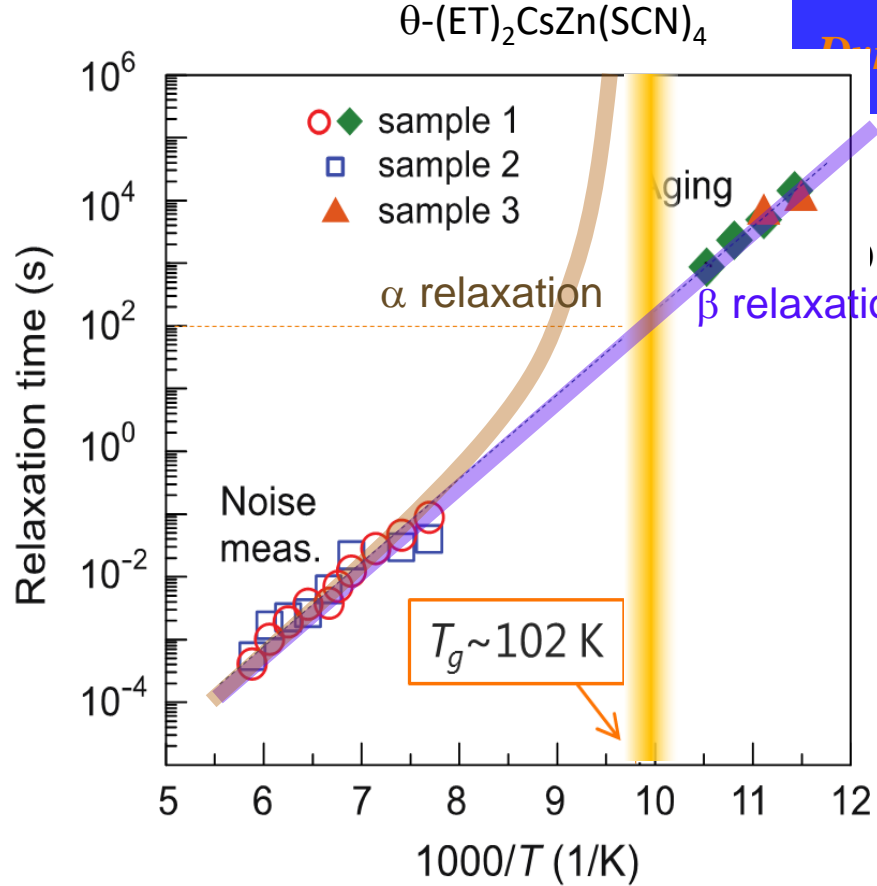


Hallmarks of Glass

- Slow dynamics
- Non-equilibrium
- Short/middle-range correlation

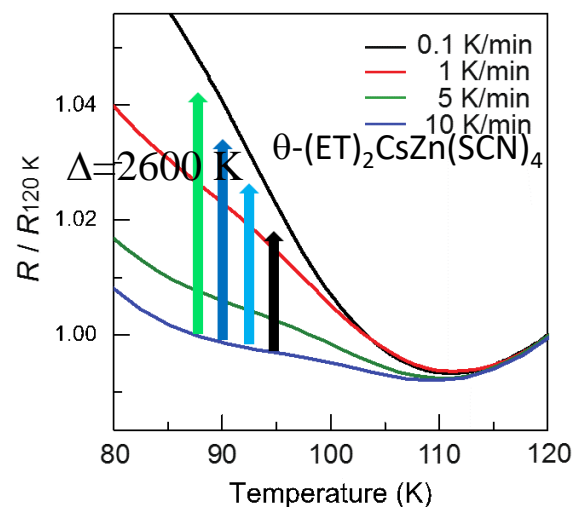
Hallmarks of Glass

Kagawa *et al.*, *Nat. Phys.* **9**, 419 (2013).
 Sato *et al.*, *PRB* **89**, 121102 (2014)
 Sato *et al.*, *JPSJ* **83**, 083602 (2014)
 Sato *et al.*, *JPSJ* **85**, 123702 (2016)



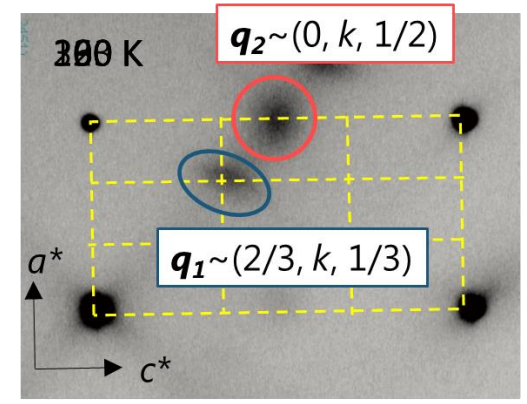
Non-equilibrium nature

ρ depends on cooling rate

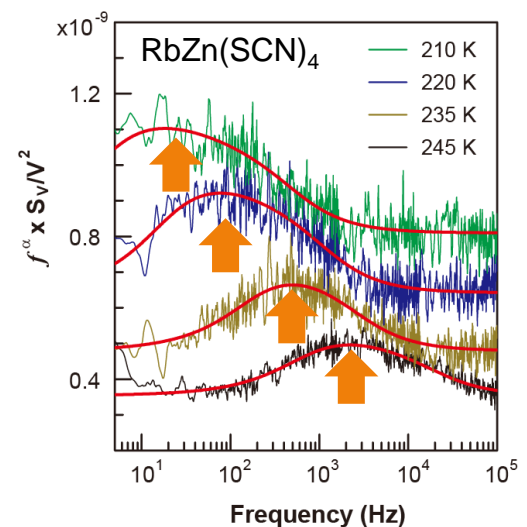
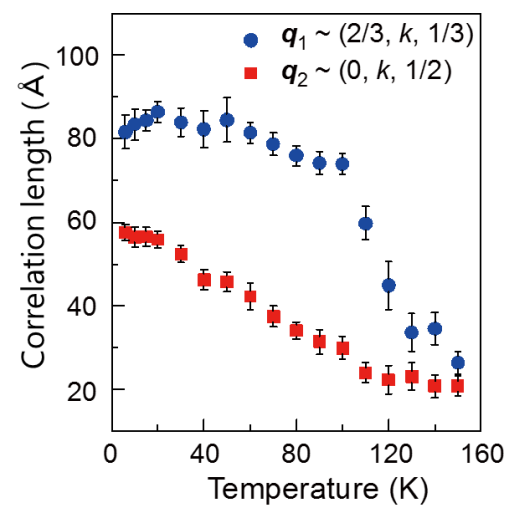


middle-range correlation

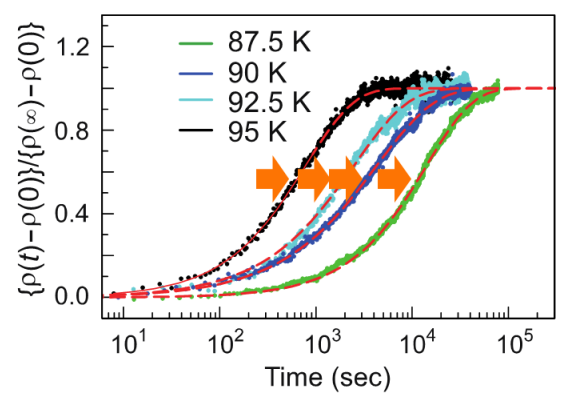
X-ray diffuse scattering



Correlation length levelling off



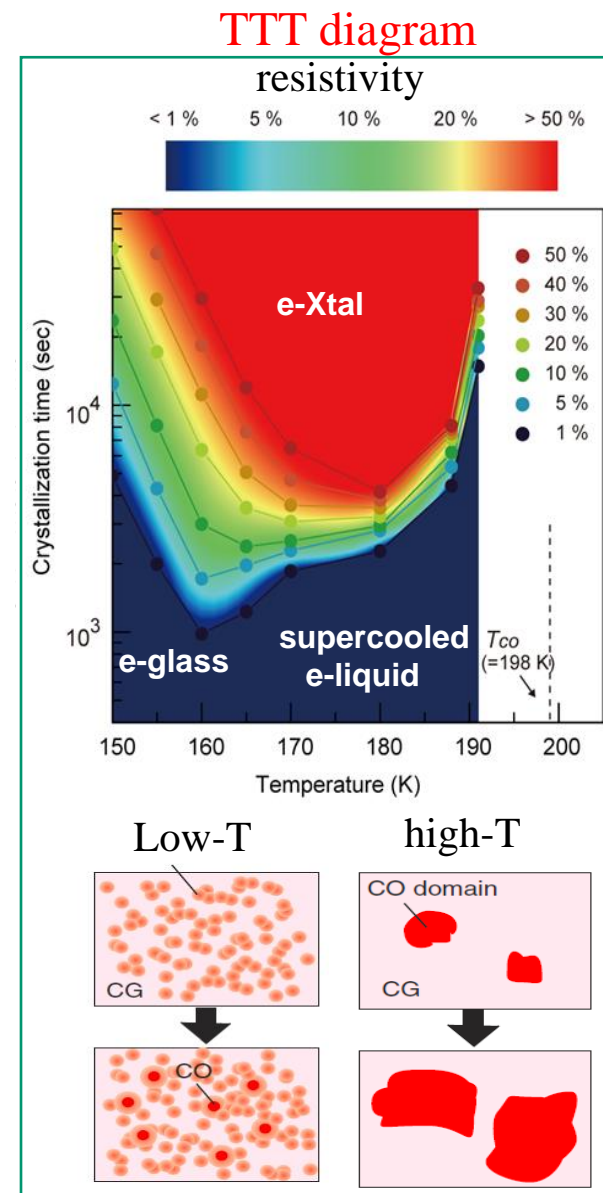
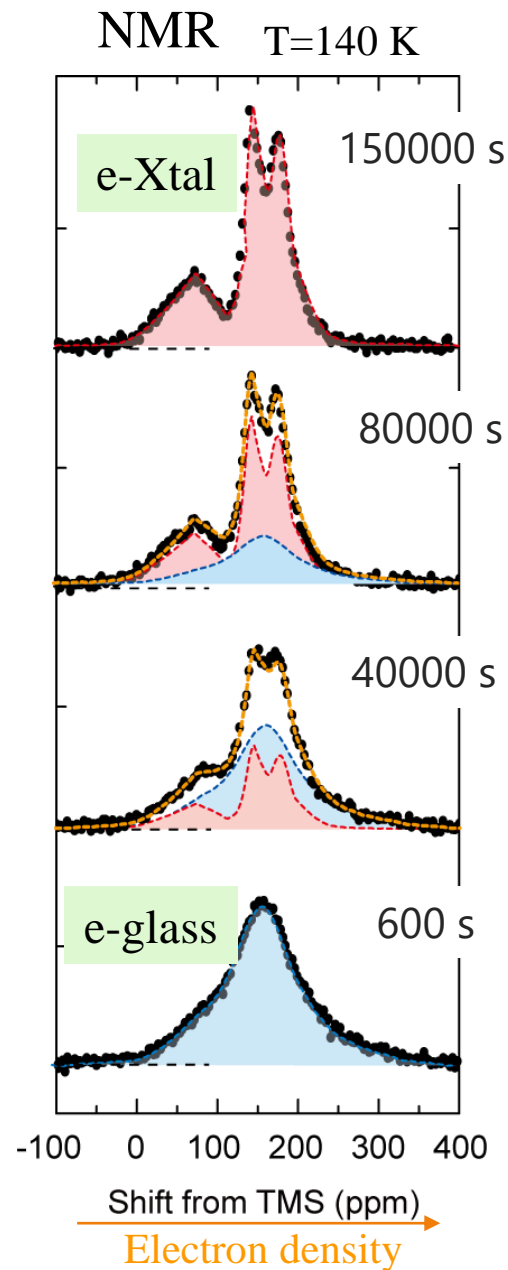
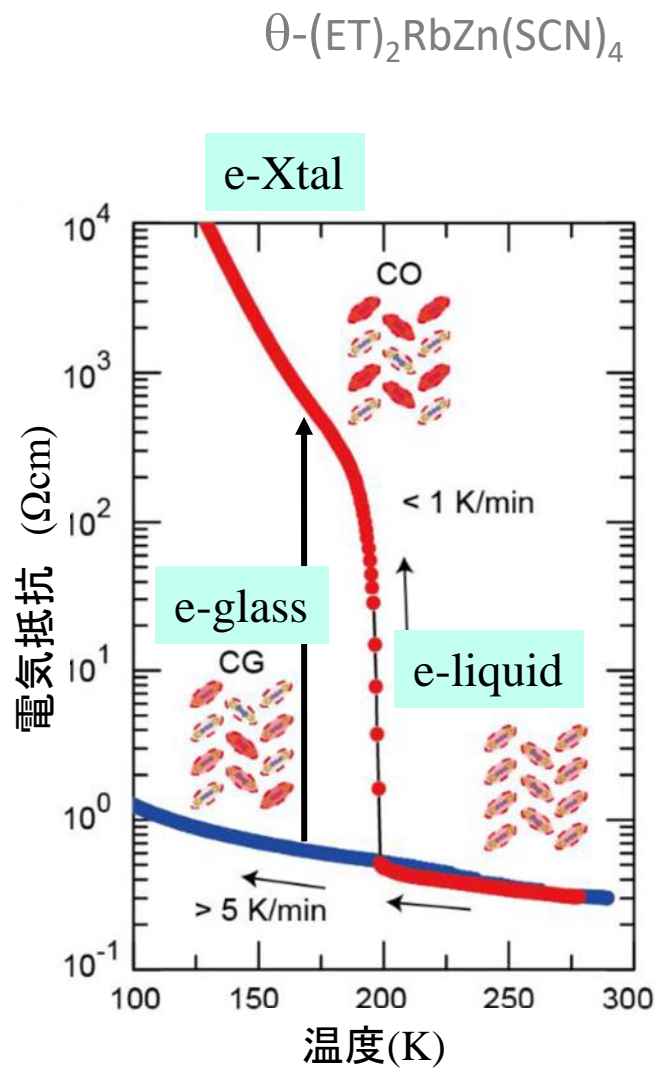
Aging



Electronic crystallization: ρ and NMR

T. Sato et al., Science 357, 1378 (2017)

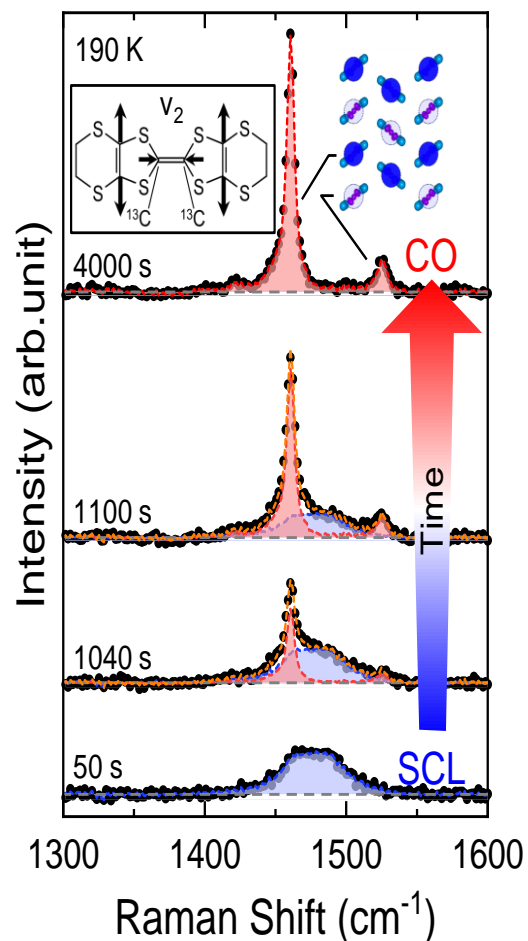
(*cf. S. Sasaki et al., Science 357, 1381 (2017)*)



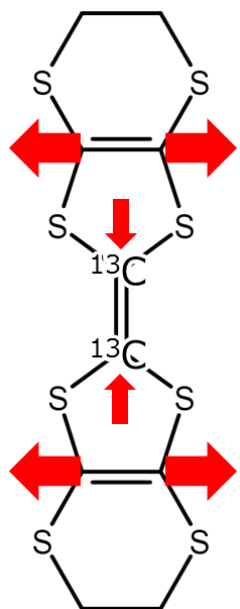
Electronic crystallization: Raman spectroscopy



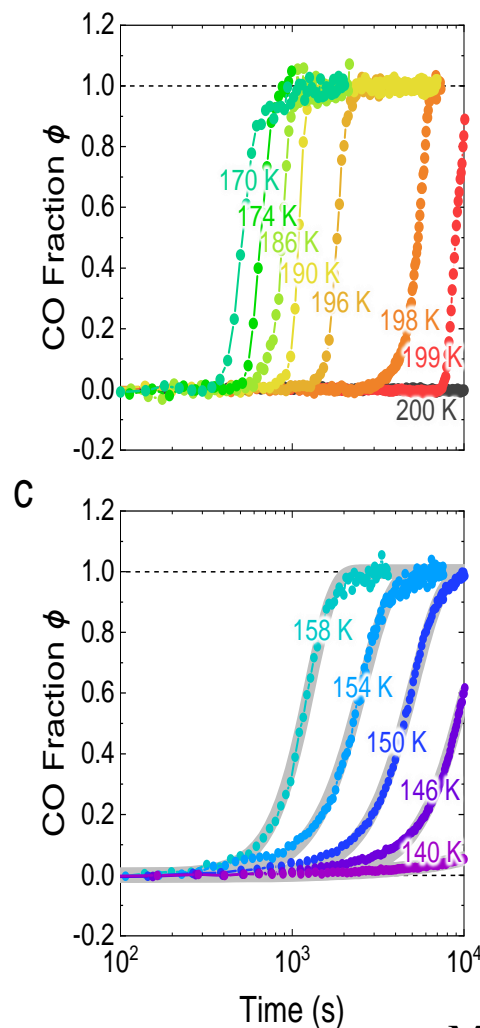
Evolution of Raman spectrum during E-crystallization



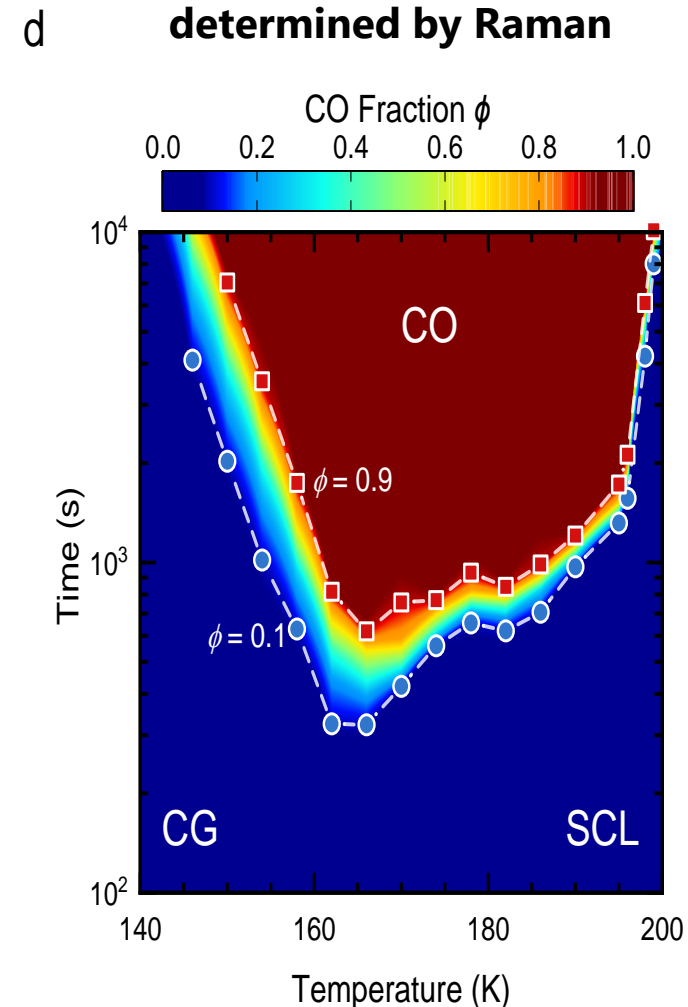
Charge-sensitive v_2 mode



Time evolution of E-Xtal fraction



TTT diagram determined by Raman



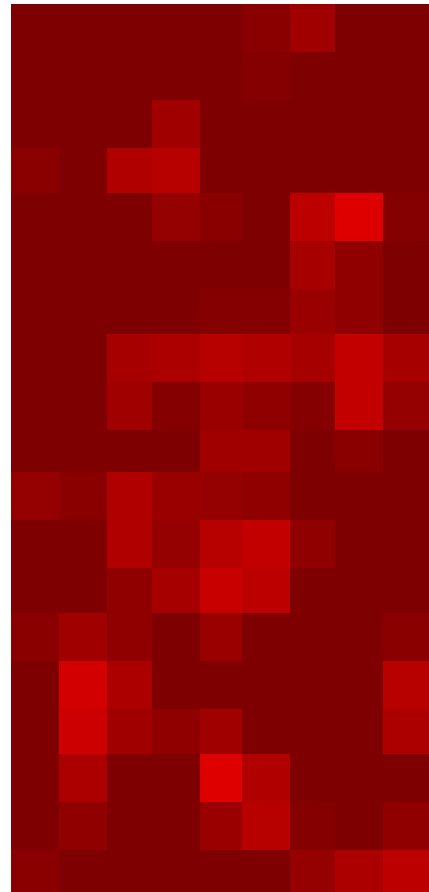
Raman imaging of E-crystallization at high T

村瀬、荒井、平川

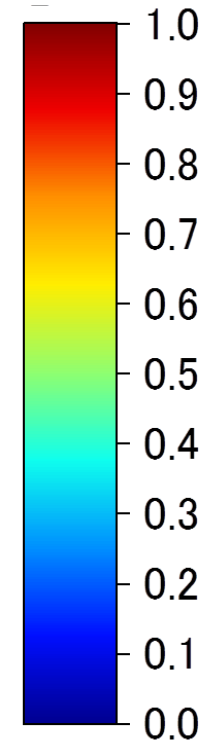
$$T_q = 195 \text{ K}$$

150 s interval
 $6.5 \times 6.5 \mu\text{m}^2/\text{pixel}$

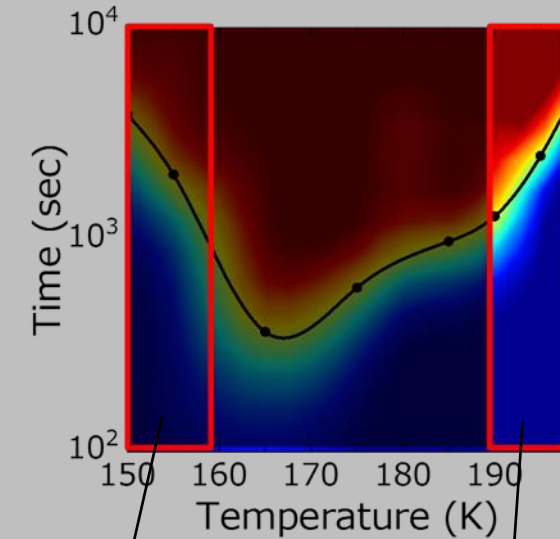

20 μm



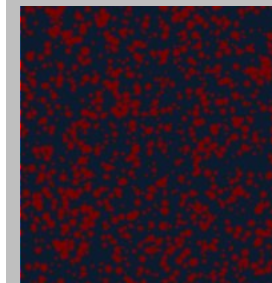
Fraction
of Xtal



**Macroscopically
inhomogeneous**

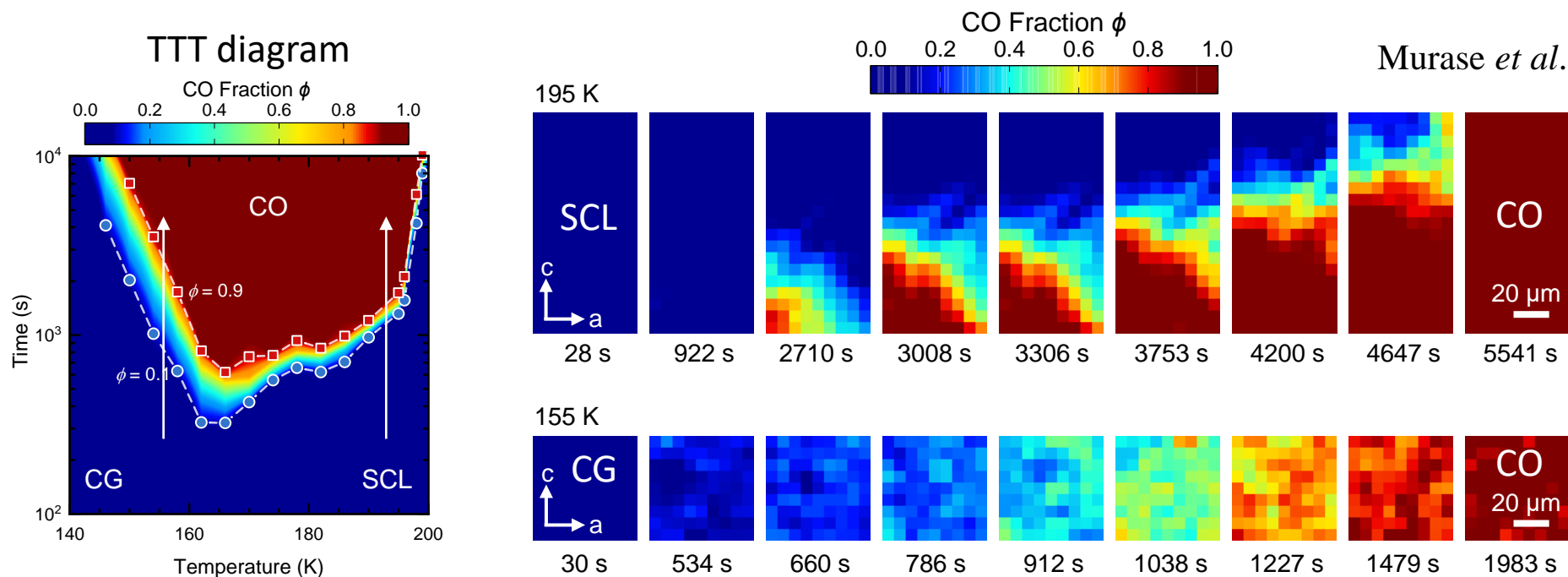


Expected
spatial profile

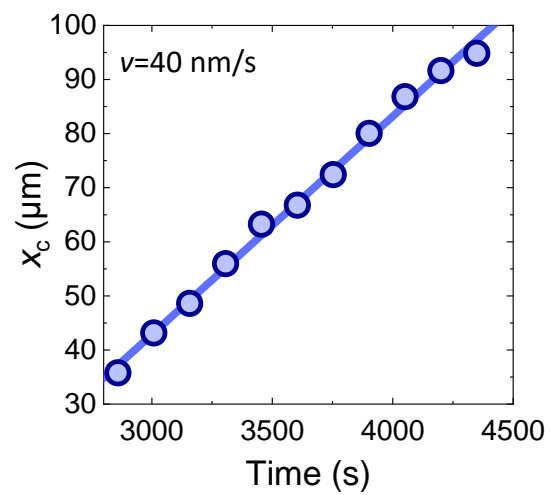
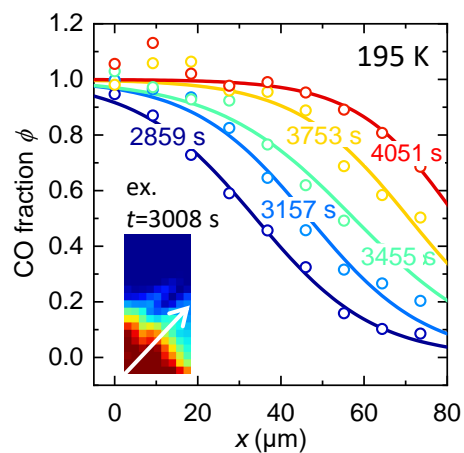


Spaciotemporal observation of electronic crystallization: classical glass

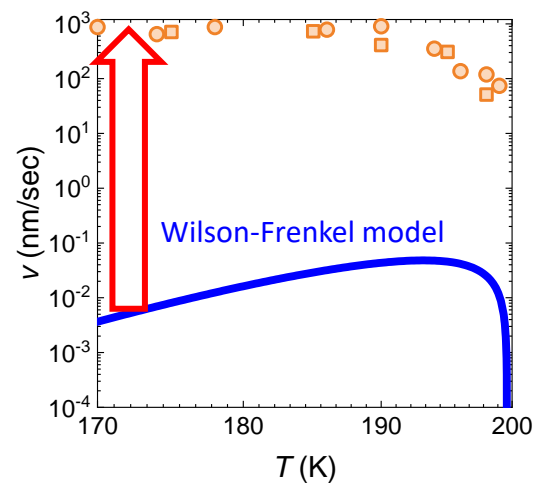
Murase *et al.*, arXiv:2201.04855



Ultrafast crystal growth: quantum effect ?



five orders of magnitude faster than expected in the classical model !



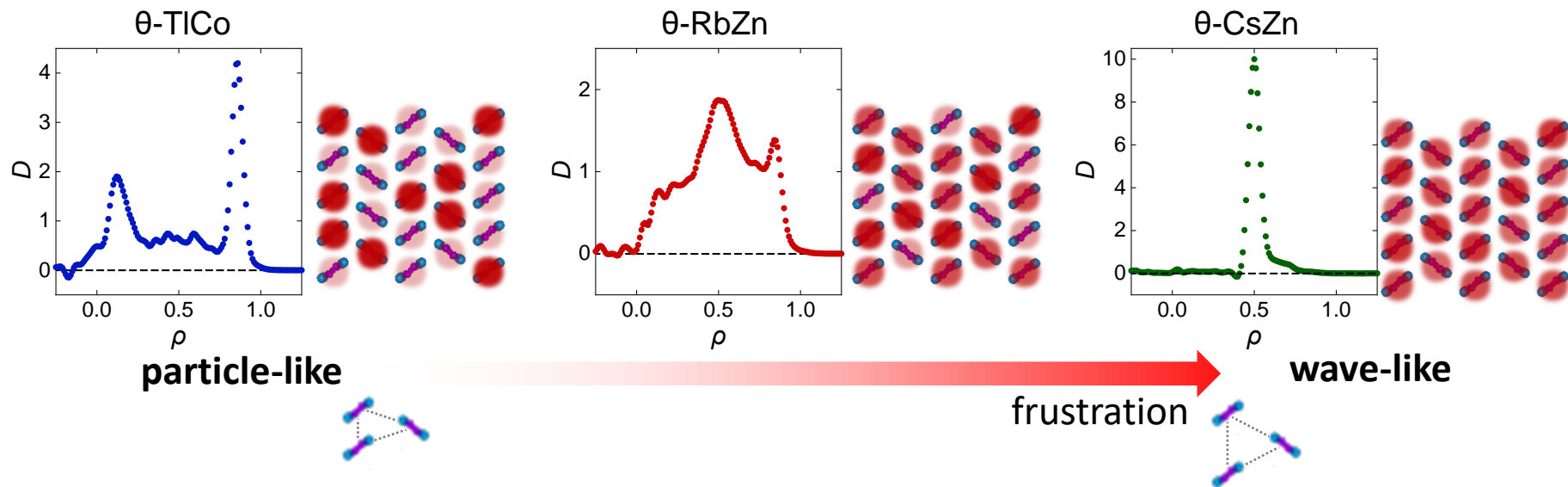
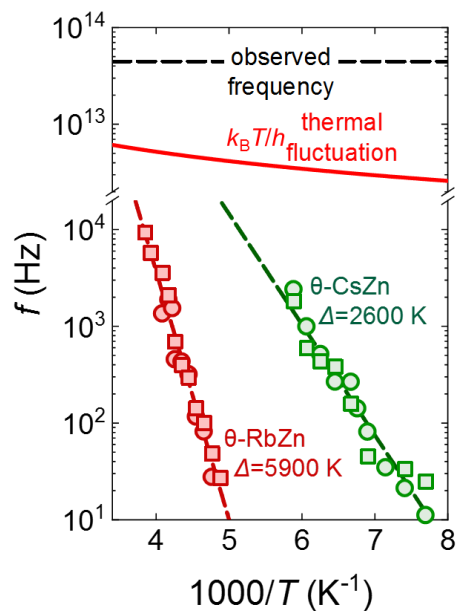
From classical to quantum charge glass

Murase *et al.*, unpublished

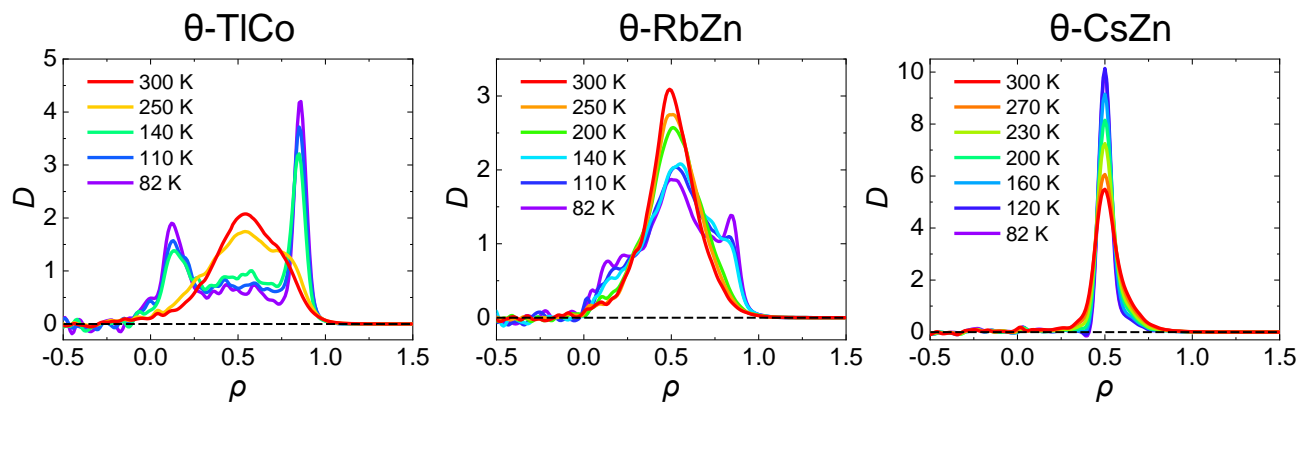
Frustration dependence of charge density in CG at 82 K

Observation time scale

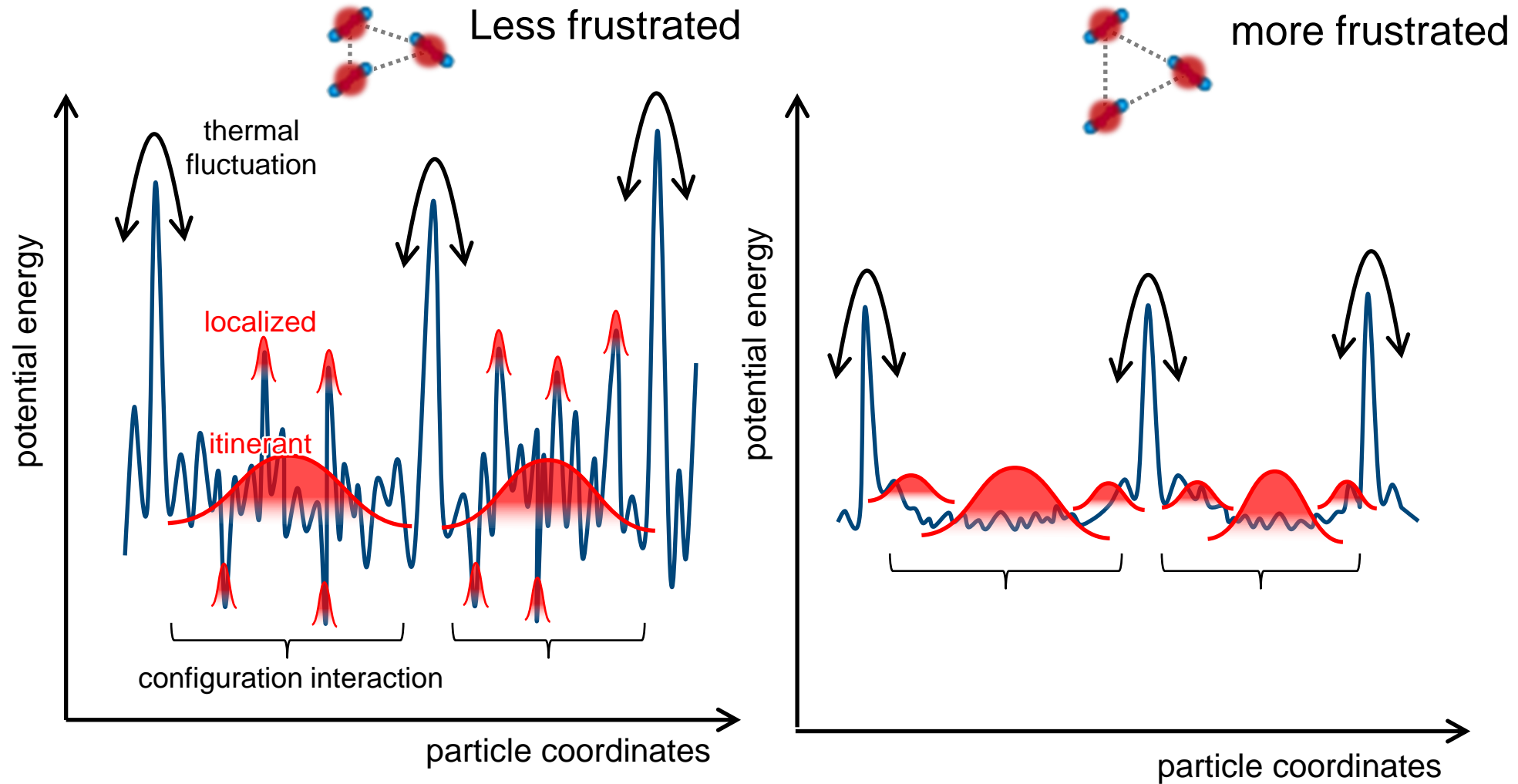
$$f_{\text{obs}} \gg f_{\text{thermal}} \gg \gg f_{\text{glass}}$$



Temperature dependence of charge density



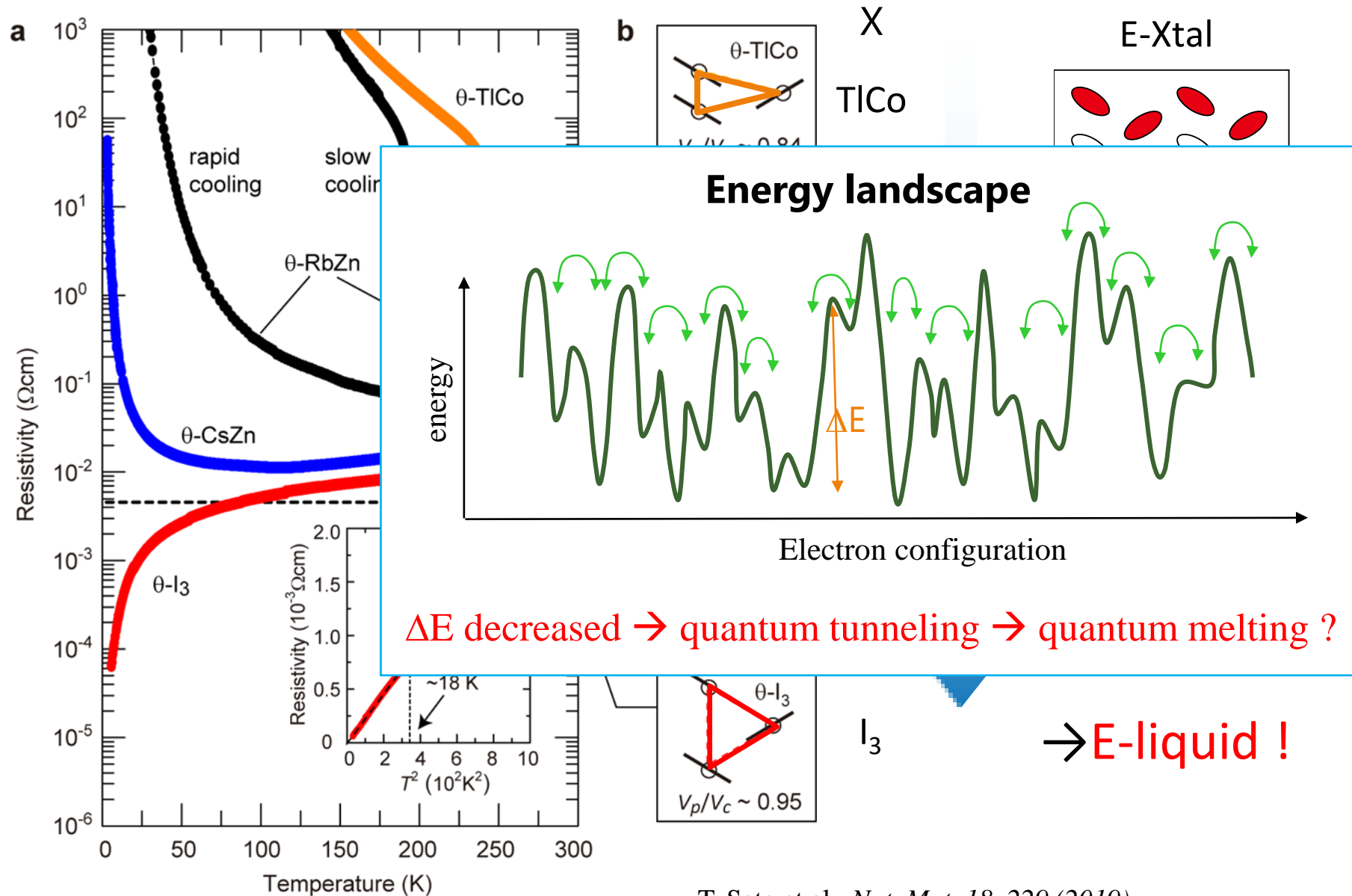
Discussion | Energy landscape



Classical glass

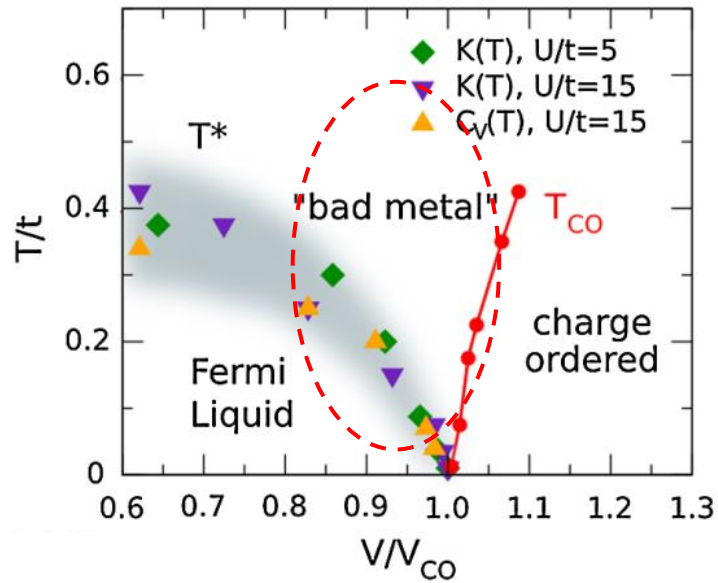
Quantum glass

Possible quantum melting of E-glass

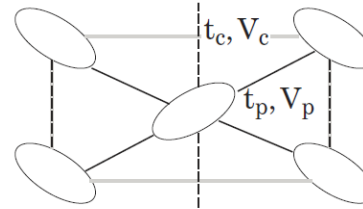


Strange metal arising from frustration-driven charge instability

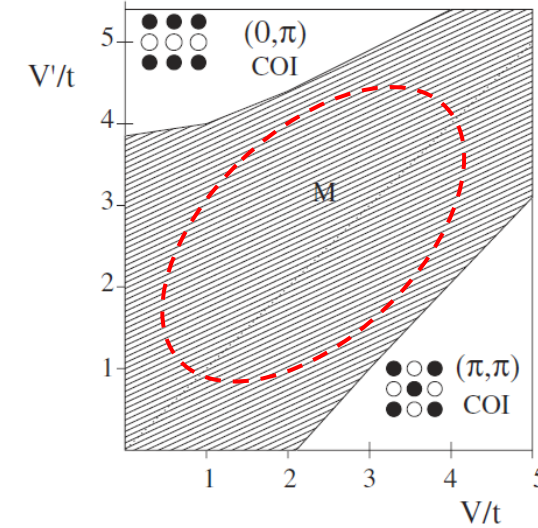
L. Cano-Cortes, et al, PRL **105**, 036405 (2010)
PRB **84**, 155115 (2011)



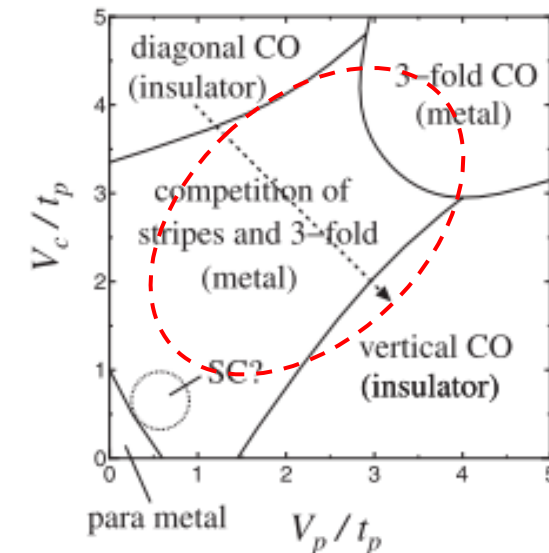
theoretical



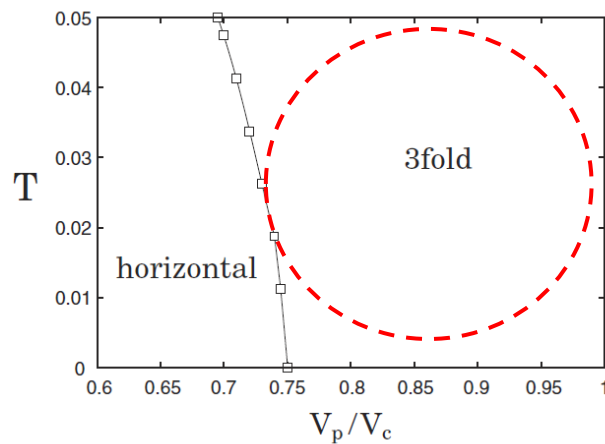
J. Merino et al, PR B **71**, 125111 (2005)



H. Watanabe, et al, JPSJ (2006)



Y. Tanaka & K. Yonemitsu JPSJ (2007)



Diverse electronic states spring from a single molecular species, ET, only by changing its arrangement

Massless Dirac electrons

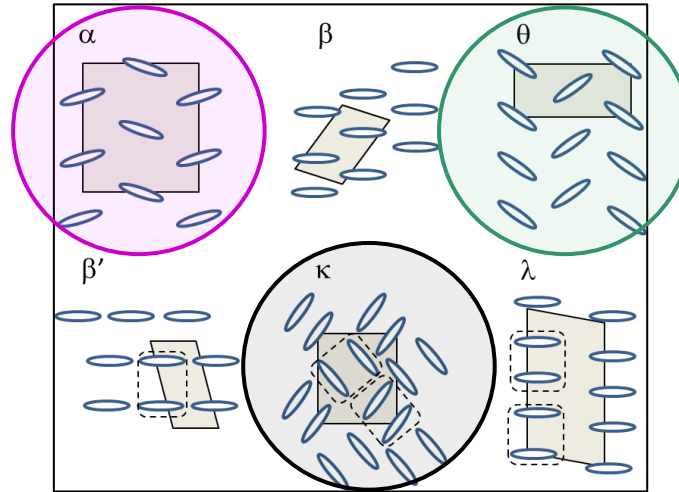
Dirac cone reshaping
Unusual spin correlation
Dynamic mass generation

Particle physics

Electronic Xtal/glass

Non-equilibrium
Slow dynamics
Crystal growth
Quantum glass

Soft matter physics



Mott physics

Quantum Mott criticality
Preformed Cooper pairs
Spin liquid
BEC-BCS crossover